Determination of nuclear deformations with an emulator for sub-barrier fusion reactions

Speaker： Zehong Liao

Collaborator： K. Hagino, S. Yoshida, K. Uzawa, Z. Long

Content

What is Low-energy sub-barrier fusion reaction?

A tunnel phenomena across the Coulomb barrier

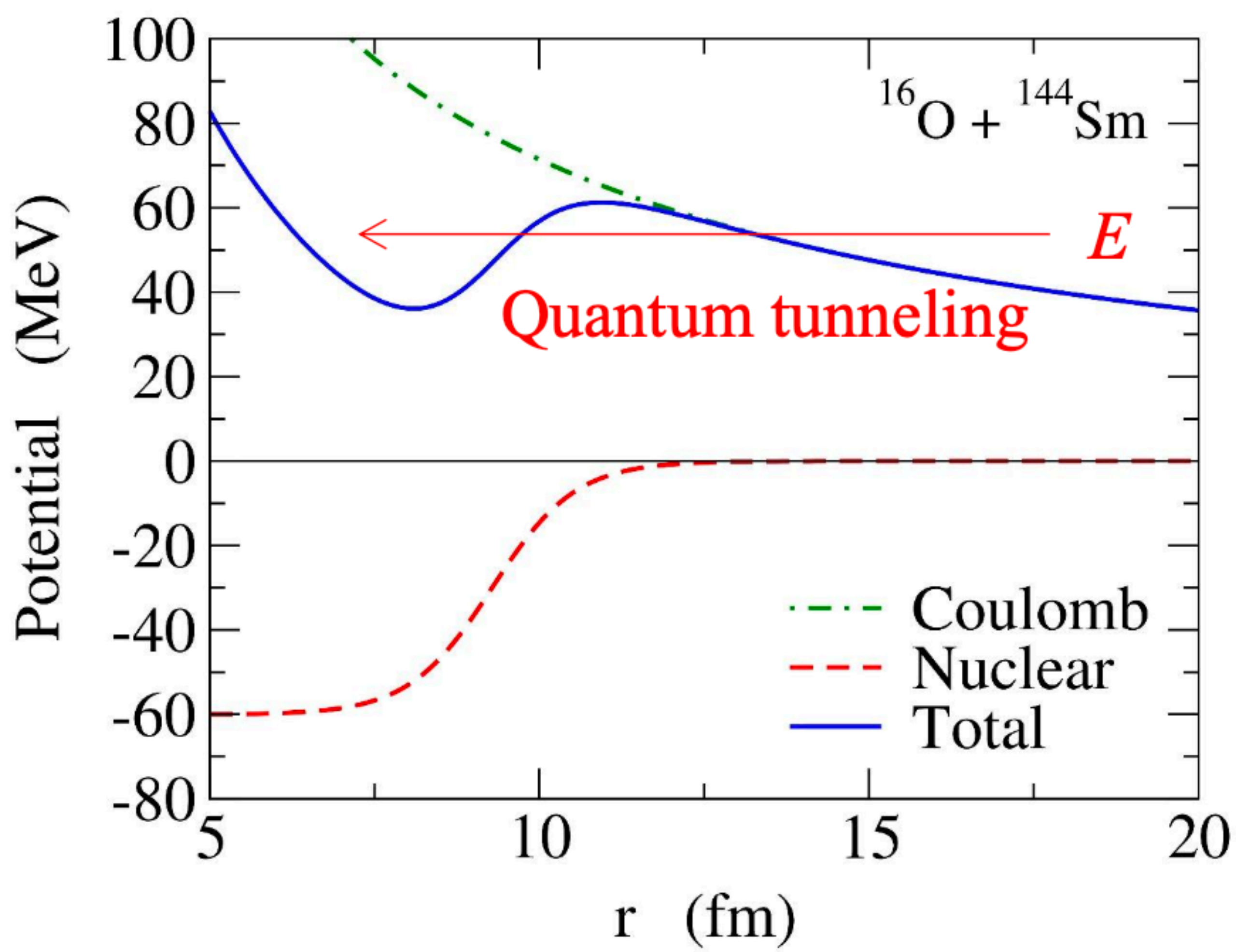

1. Coulomb interaction
   long range, repulsion
2. Nuclear interaction
   short range, attraction

⇓

Potential barrier (Coulomb barrier)

Fusion: takes place by overcoming the barrier

the barrier height → defines the energy scale of a system

Fusion reactions at energies around the Coulomb barrier

K. Hagino and N. Takigawa, PTP128 (2012) 1061

What is Low-energy sub-barrier fusion reaction?：

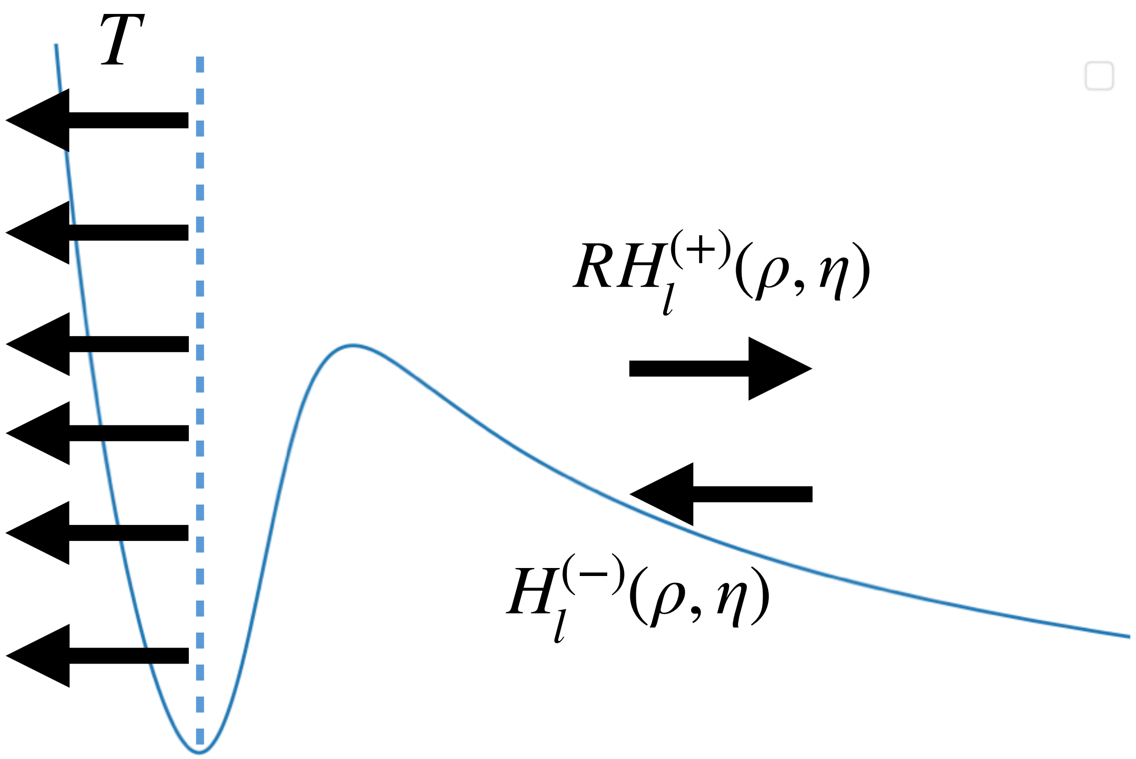

The boundary conditions are thus expressed as

$$\psi(x) \to H_J^{(-)}(k_n r)\,\delta_{n,0} + R\,H_J^{(+)}(k_n r) \quad \text{for } r > r_{\max}$$
$$\to T\,e^{-ikr} \quad \text{for } r < r_{\min}$$

$$\left[-\frac{\hbar^2}{2\mu}\frac{d^2}{dr^2} + \frac{J(J+1)\hbar^2}{2\mu r^2} + V_N^{(0)}(r) + \frac{Z_P Z_T e^2}{r} - E\right]\psi_n(r) = ($$

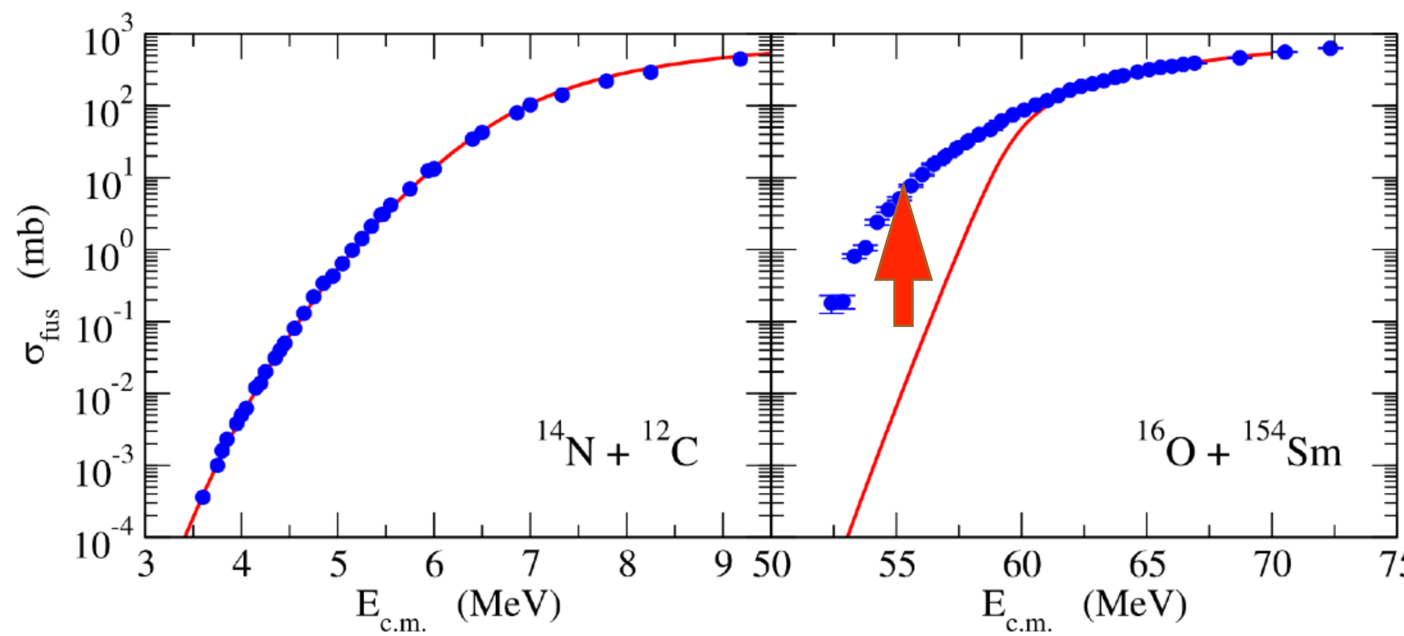

Penetration Probability: $T_J = 1 - |R|^2$

Fusion cross section: $\sigma_{\text{fus}}(E) = \frac{2\pi}{k^2}\sum_J (2J+1)T(E,J)$

- **Work well for relatively light systems**
- **Work not well for heavy systems at low energies**

K. Hagino and N. Takigawa, PTP128 (2012) 1061

How to explain the phenomenon：

- several nuclear shapes

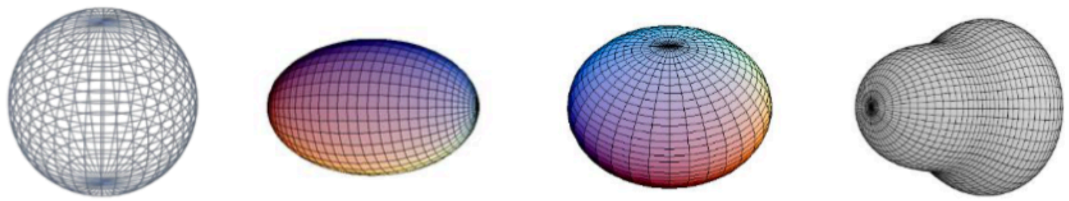

- several surface vibrations

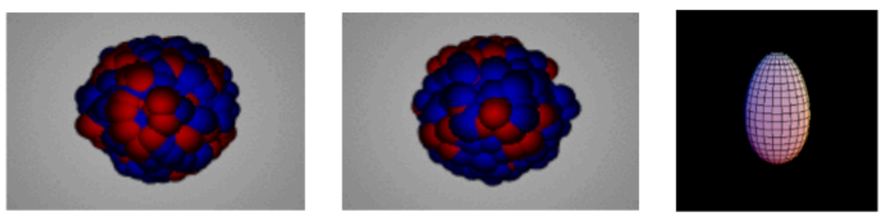

several modes and adiabaticities

- several types of nucleon transfers

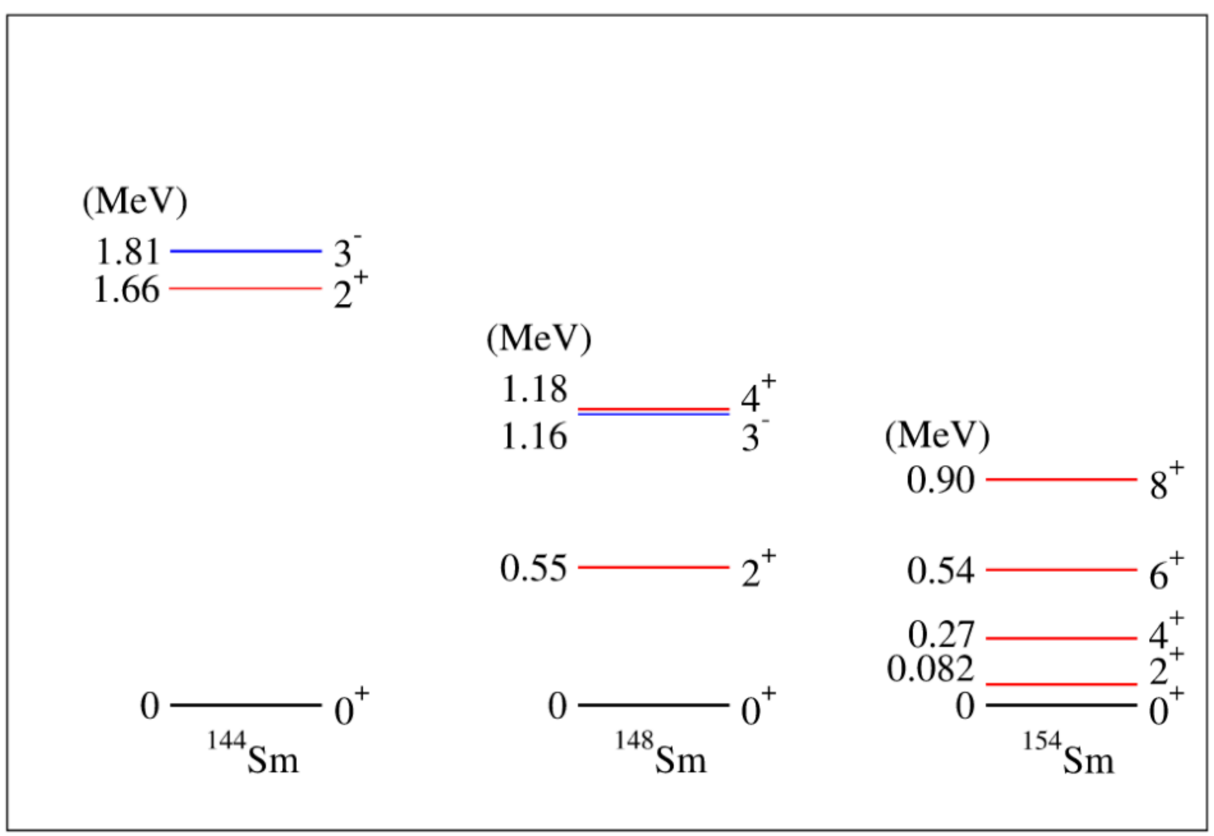

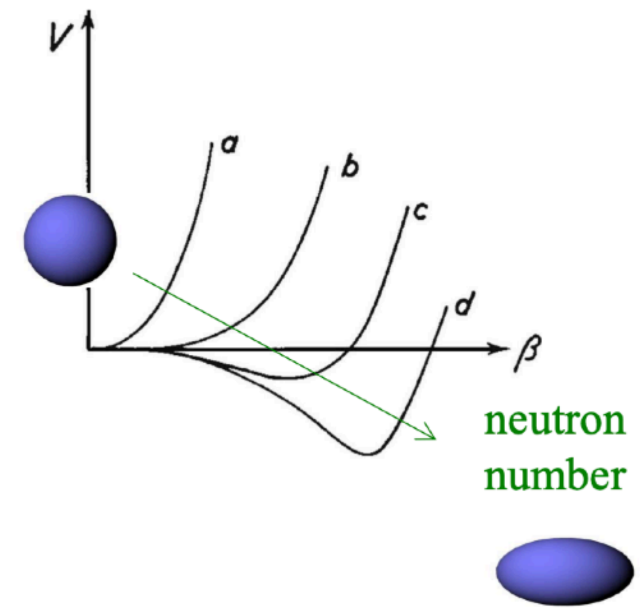

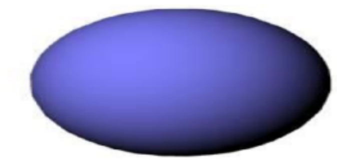

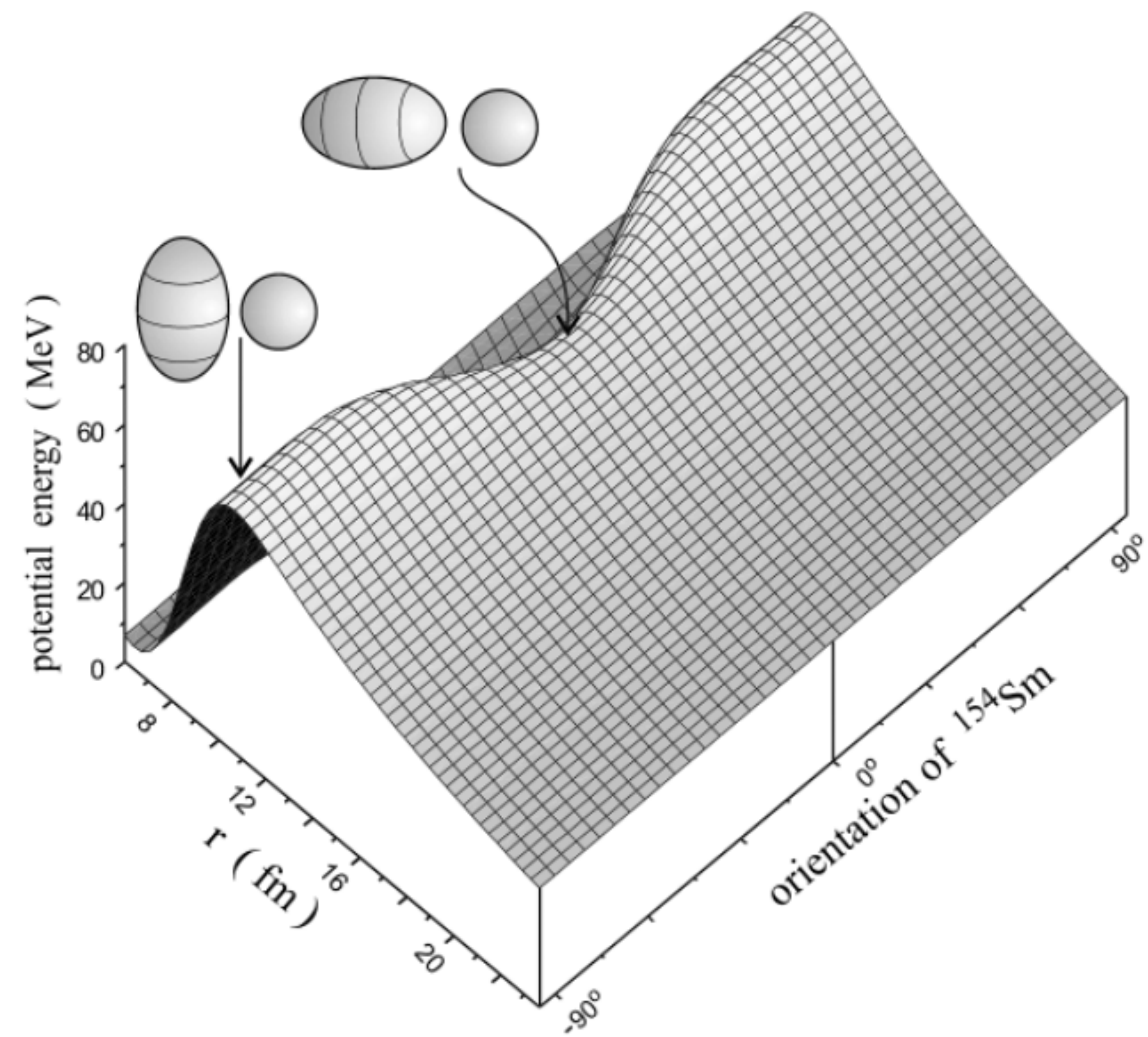

K. Hagino and N. Takigawa, PTP128 (2012) 1061

How to explain the phenomenon in classical picture：

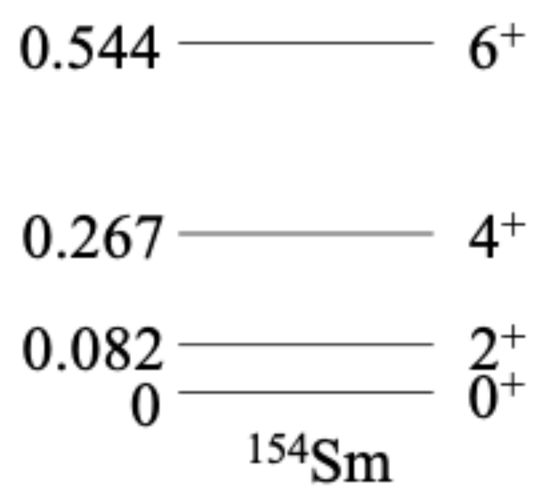

$$\sigma_{\mathrm{fus}}(E) = \int_0^1 d(\cos\theta)\sigma_{\mathrm{fus}}(E,\theta)$$

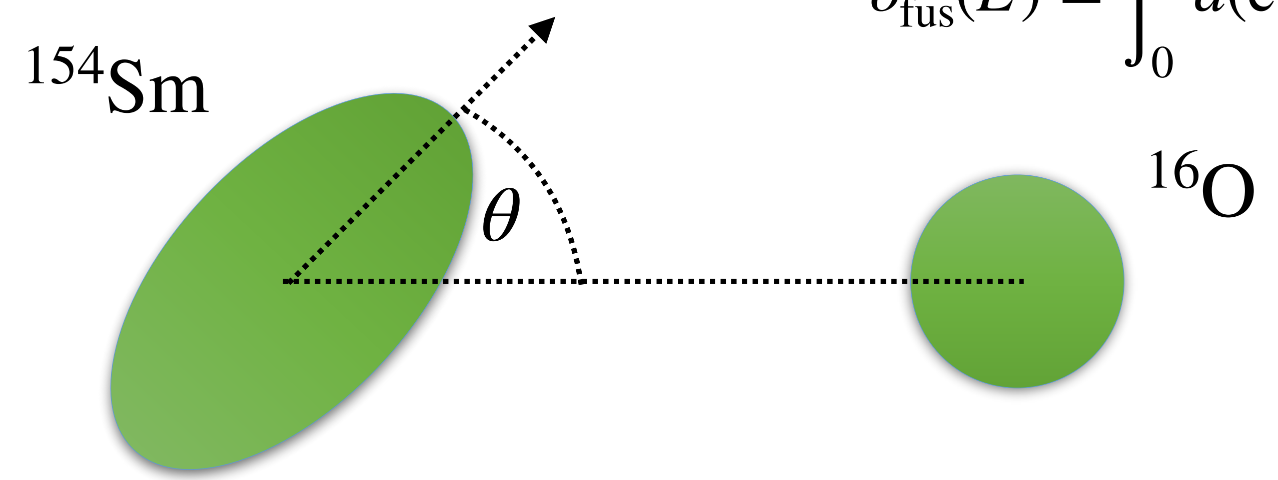

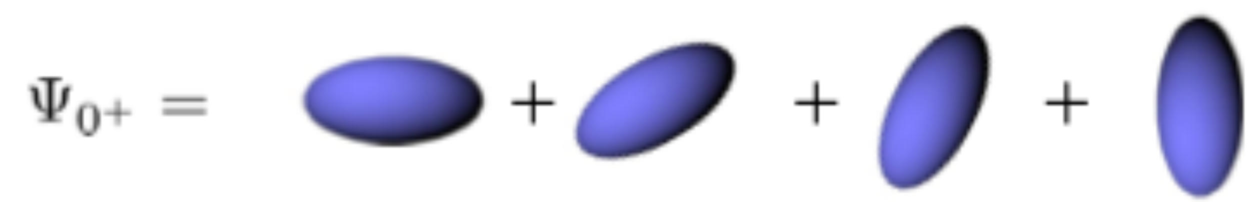

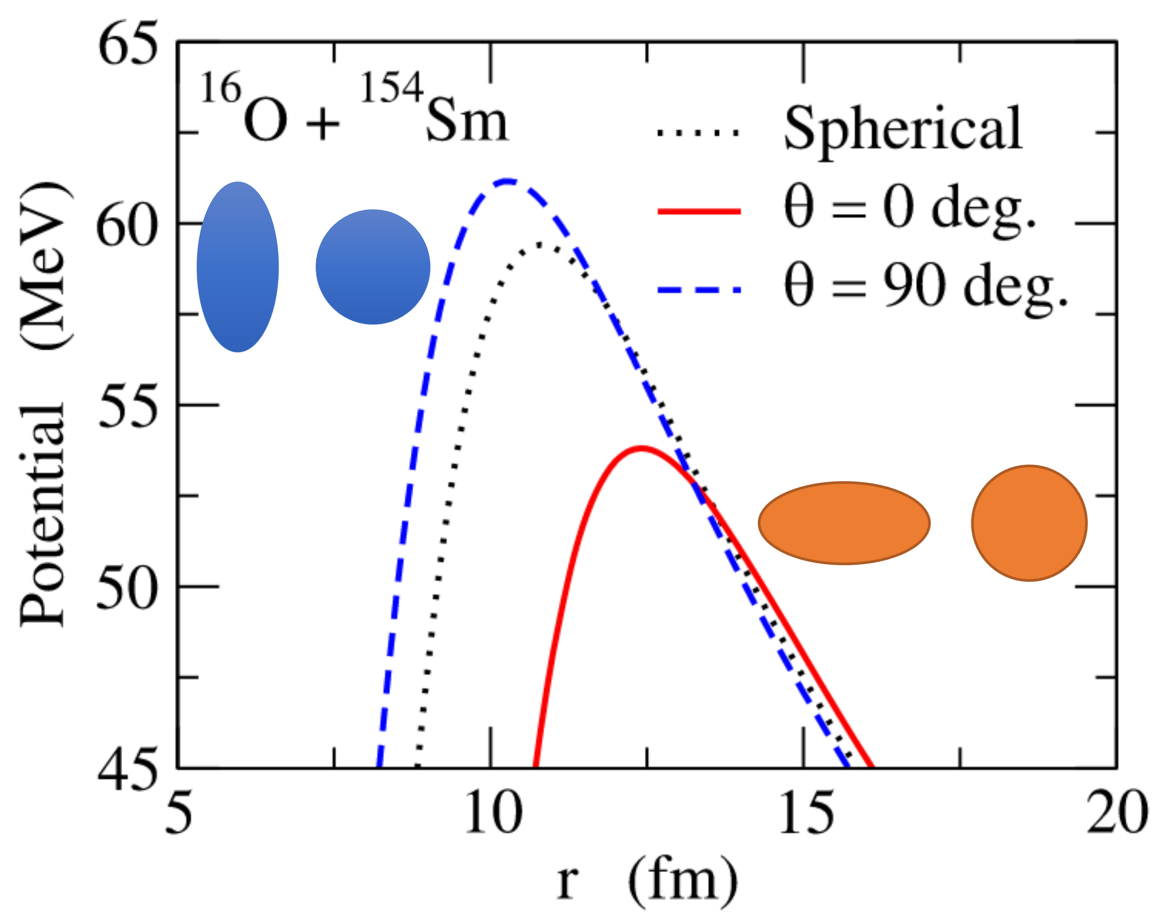

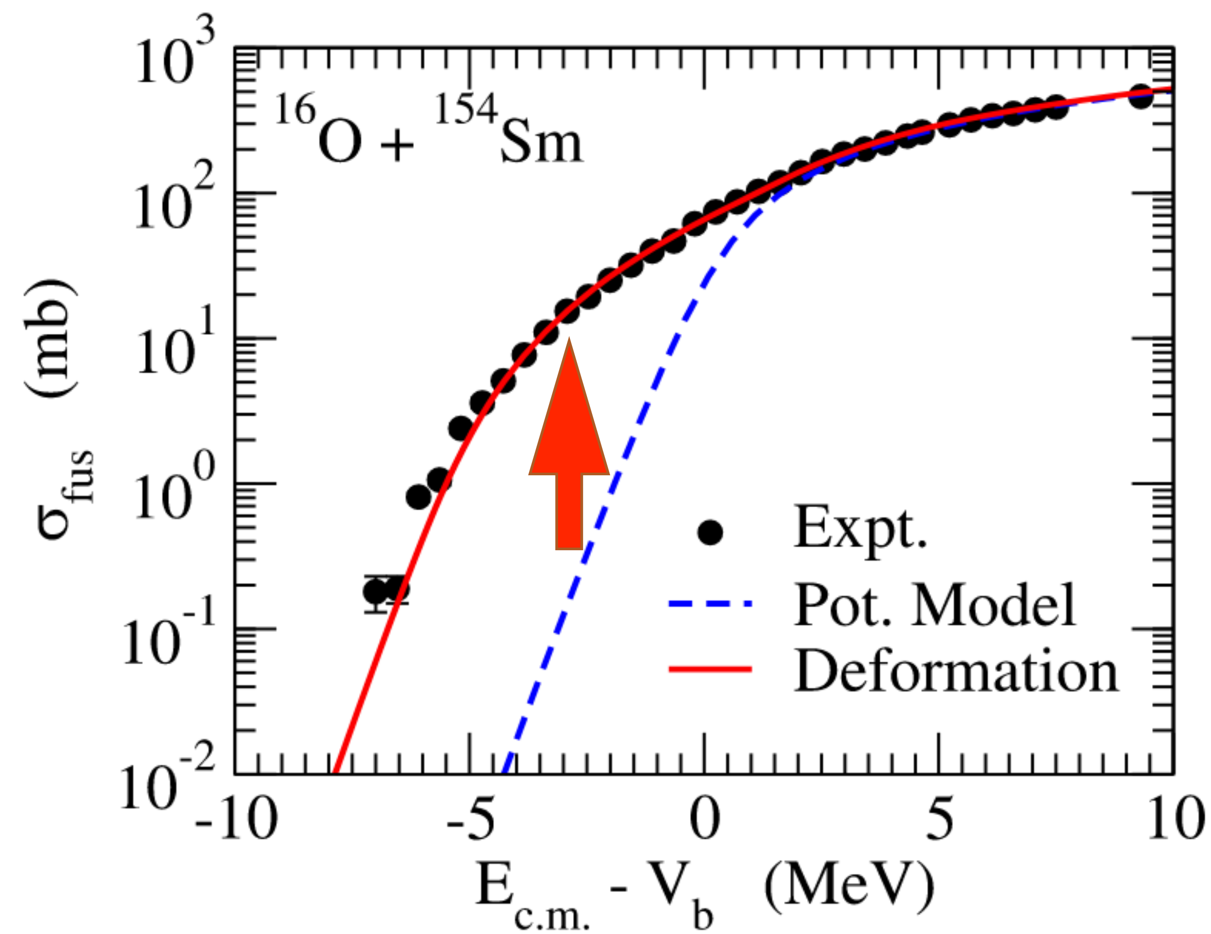

K. Hagino and N. Takigawa, PTP128 (2012) 1061

Coupling between rel. and intrinsic motions

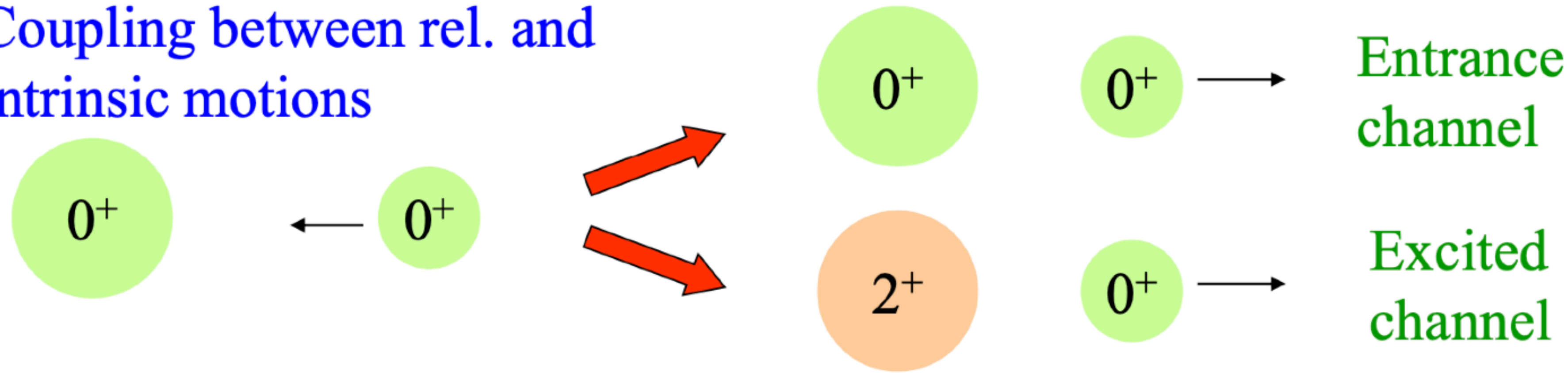

$$H = -\frac{\hbar^2}{2\mu}\nabla^2 + V_0(r) + H_0(\xi) + V_{\rm coup}(\boldsymbol{r},\xi)$$

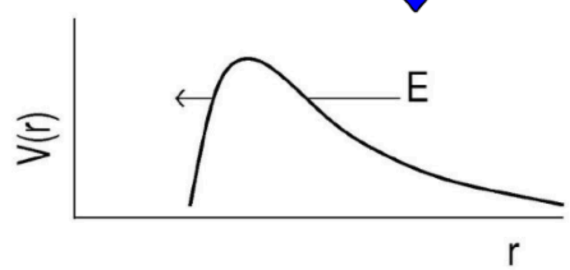

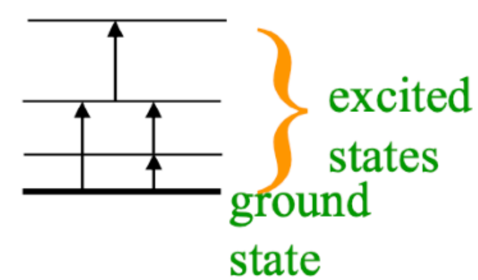

$$H_0(\xi)\phi_k(\xi) = \epsilon_k\,\phi_k(\xi)$$

The total, three-channels Hamiltonian matrix

$$H = \begin{pmatrix} 2t+V_0(r_0) & -t & 0 & \cdots \\ -t & 2t+V_0(r_0) & -t & \cdots \\ 0 & -t & 2t+V_0(r_0) & \cdots \\ \vdots & \vdots & \vdots & \ddots \end{pmatrix} + \begin{pmatrix} 0 & 0 & 0 & \cdots \\ 0 & E(2^+) & 0 & \cdots \\ 0 & 0 & E(4^+) & \cdots \\ \vdots & \vdots & \vdots & \ddots \end{pmatrix} + \begin{pmatrix} V_{00}(r_0) & V_{01}(r_0) & V_{02}(r_0) & \cdots \\ V_{10}(r_0) & V_{11}(r_0) & V_{12}(r_0) & \cdots \\ V_{20}(r_0) & V_{21}(r_0) & V_{22}(r_0) & \cdots \\ \vdots & \vdots & \vdots & \ddots \end{pmatrix}$$

For convenient, I just show the element where r = r_o

$$V_{\rm nm}(r_0) = V^{(C)}_{\rm nm} + V^{(N)}_{\rm nm}(r_0)$$

K. Hagino and N. Takigawa, PTP128 (2012) 1061

How to explain the phenomenon in coupled channel model (CCFULL):

Coupling between rel. and intrinsic motions

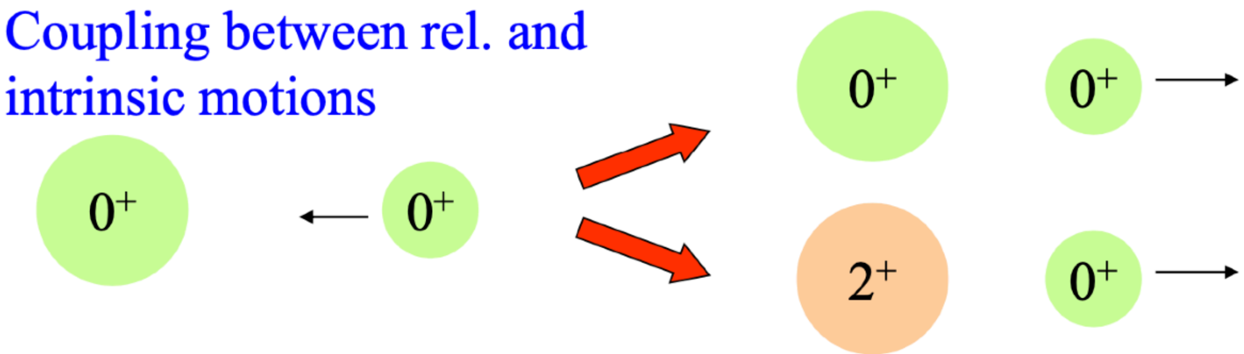

Entrance channel

Excited channel

$$H = -\frac{\hbar^2}{2\mu}\nabla^2 + V_0(r) + H_0(\xi) + V_{\rm coup}(\boldsymbol{r}, \xi)$$

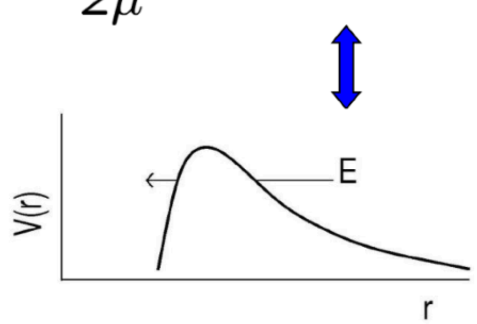

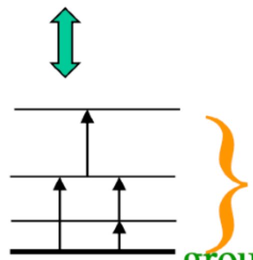

$$H_0(\xi)\phi_k(\xi) = \epsilon_k\,\phi_k(\xi)$$

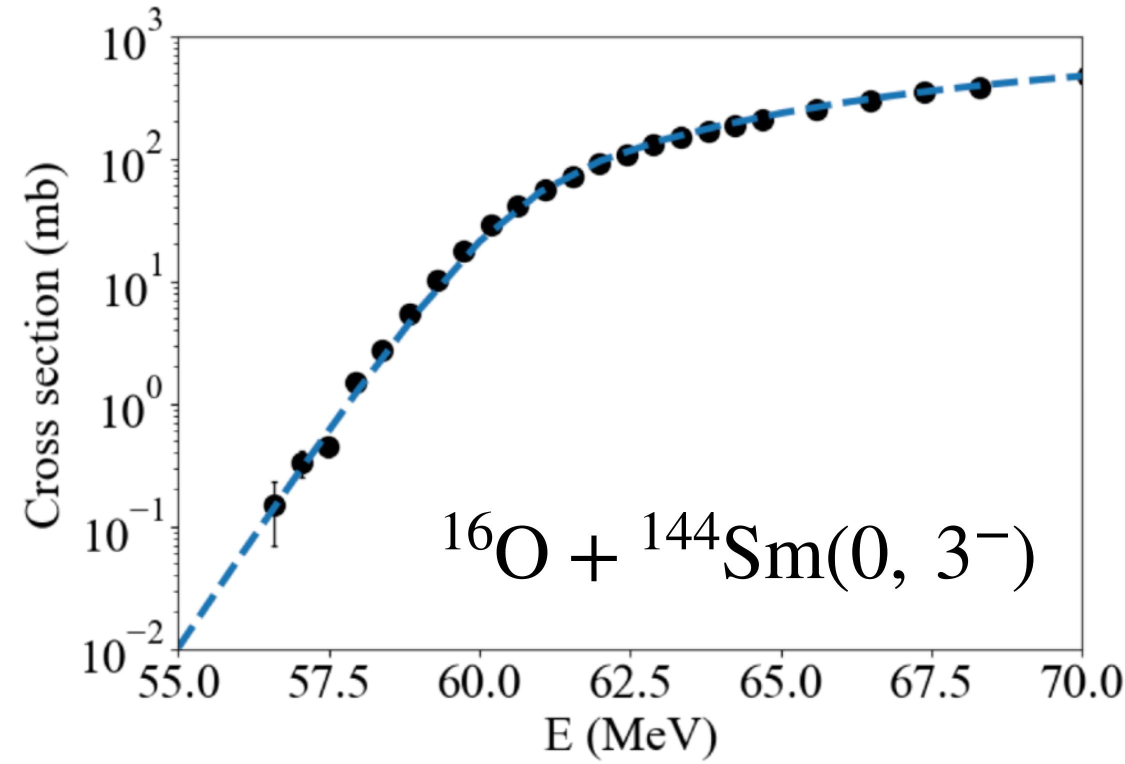

$$\left[-\frac{\hbar^2}{2\mu}\frac{d^2}{dr^2} + \frac{J(J+1)\hbar^2}{2\mu r^2} + V_N^{(0)}(r) + \frac{Z_P Z_T e^2}{r} + \epsilon_n - E\right]\psi_n(r) + \sum_m V_{nm}(r)\psi_m(r) = 0,$$

$$V_{\rm nm}(r_0) = V_{\rm nm}^{(C)} + V_{\rm nm}^{(N)} \qquad \hat{O} = \beta_2 R_T Y_{20} + \beta_4 R_T Y_{40}$$

$$\langle I'0\,|\,V^N\,|\,I0\rangle = \langle I'0\,|\,V_N(r,\hat{O})\,|\,I0\rangle - V_N^0(r)\delta_{n,m}$$

$$\langle I'0\,|\,V^C\,|\,I0\rangle = \left\langle I'0\,\middle|\,\frac{3Z_P Z_T e^2}{5}\frac{R_T^2}{r^3}\beta_2 Y_{20}\,\middle|\,I0\right\rangle + \left\langle I'0\,\middle|\,\frac{3Z_P Z_T e^2}{9}\frac{R_T^4}{r^5}\beta_4 Y_{40}\,\middle|\,I0\right\rangle$$

K. Hagino and N. Takigawa, PTP128 (2012) 1061

Rich properties:

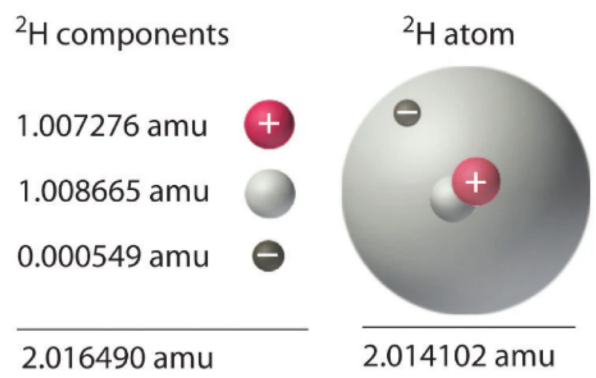

Mass

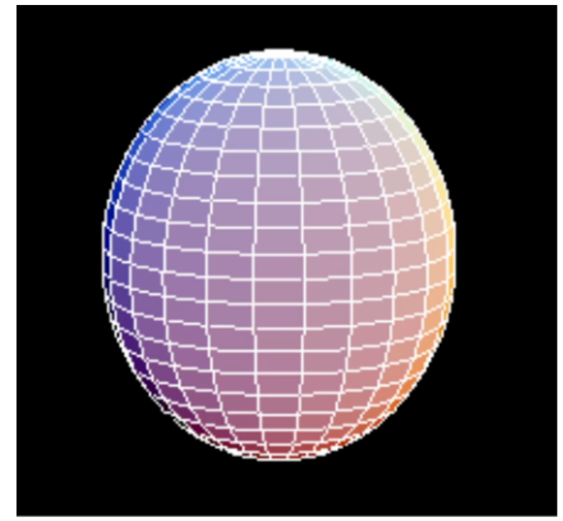

Collective mode

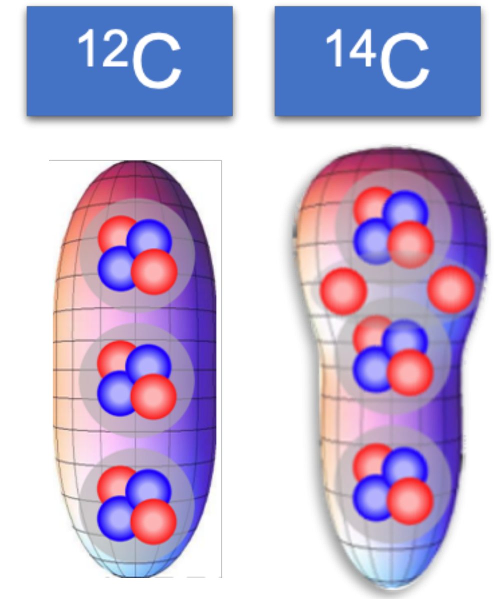

Exotic structure

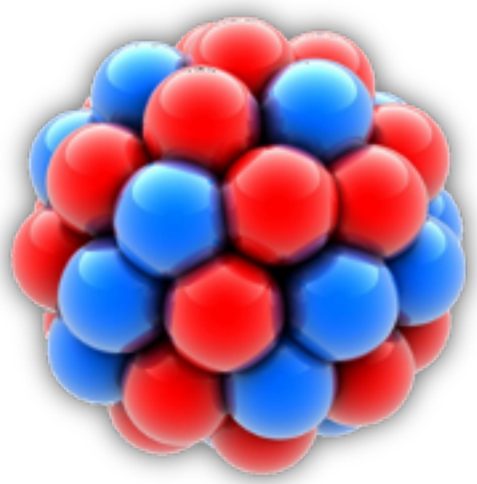

Quantum many-body systems

DFT determines these properties:

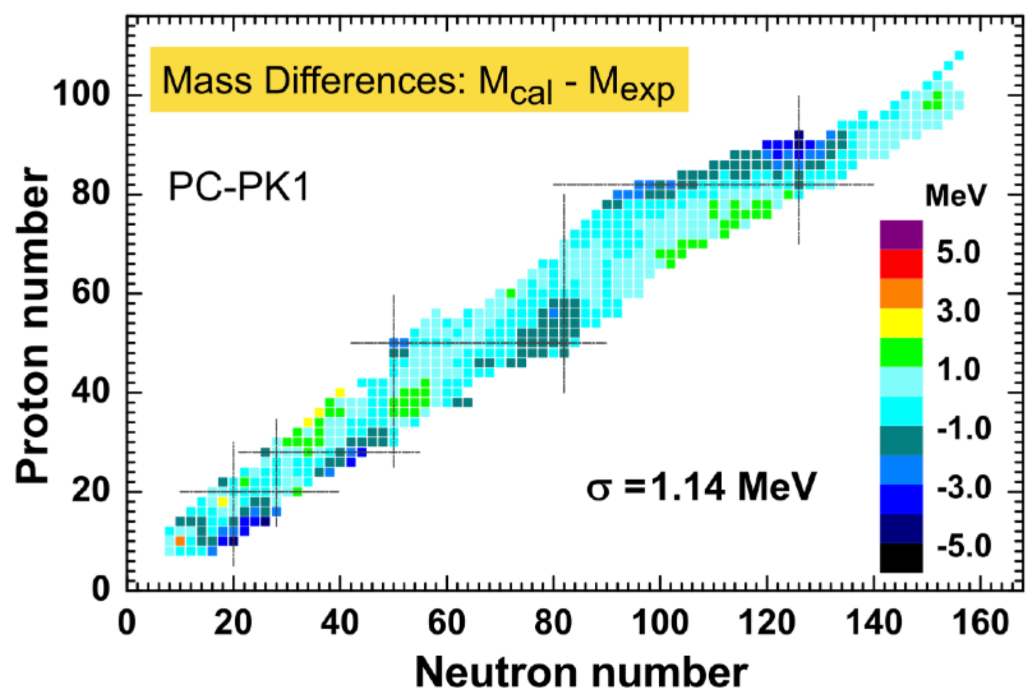

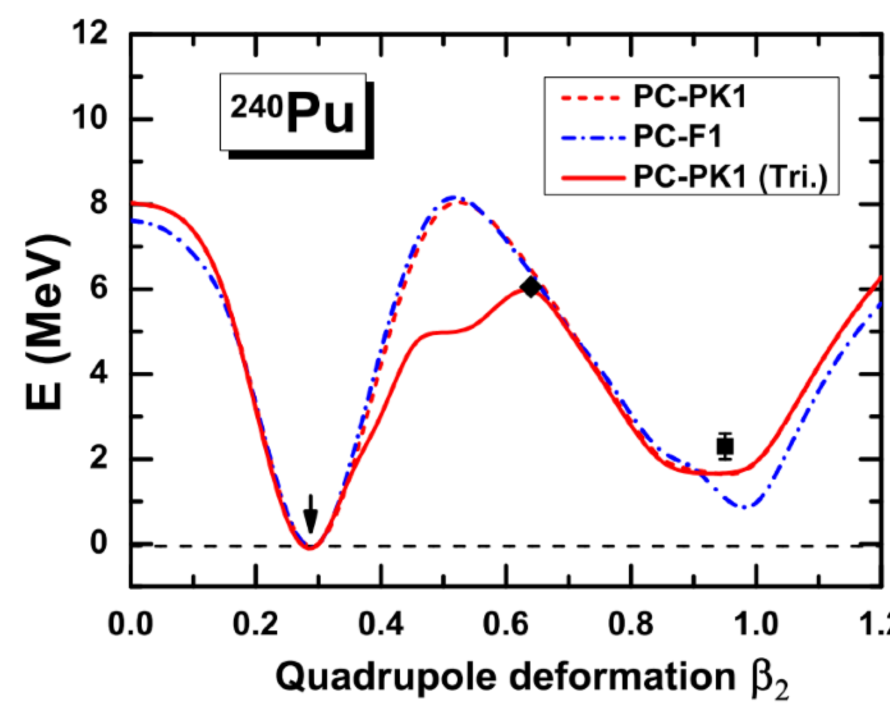

Meng, J., Zhao, P. Relativistic density functional theory in nuclear physics. AAPPS Bull. 31, 2 (2021)

Probing nuclear shapes in Relativistic H.I. collisions

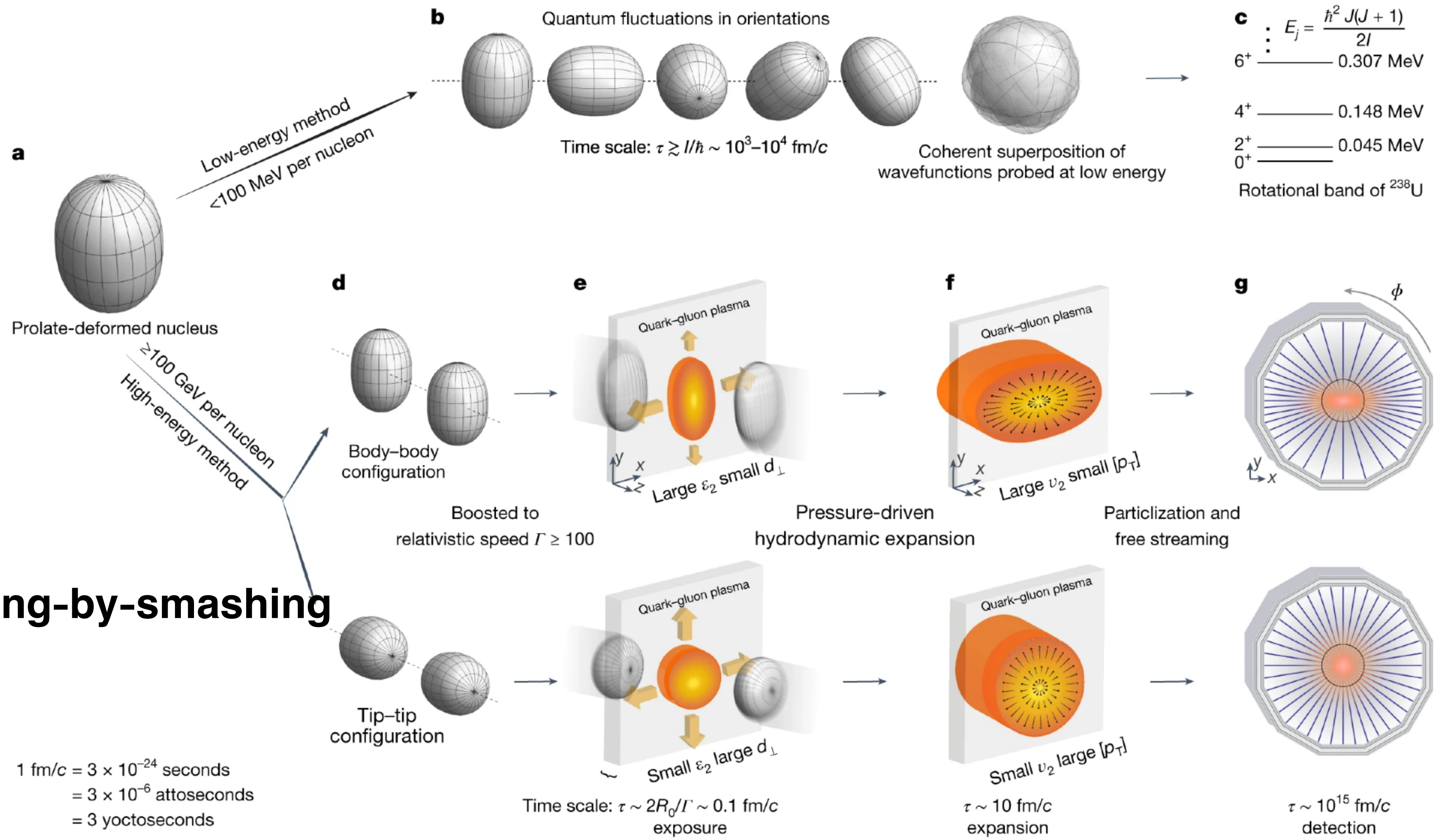

imaging-by-smashing

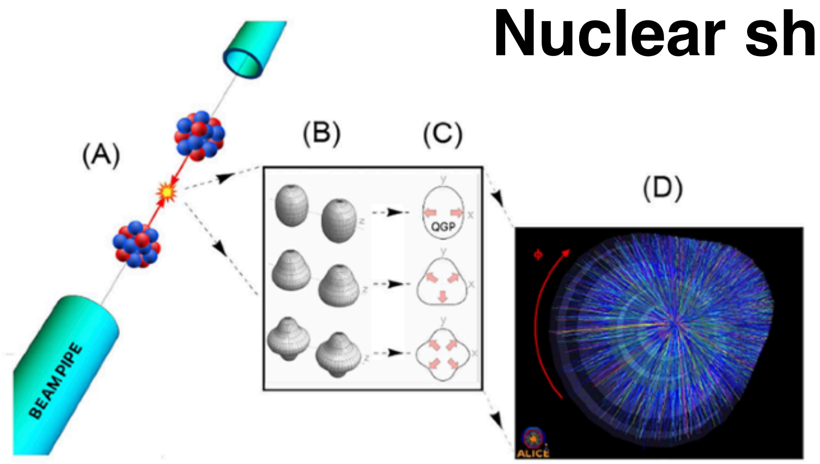

Nuclear shapes are encoded during quark-gluon plasma formation and evolution

M.I. Abdulhamid et al. (STAR collaboration) Nature 635, 67 (2024)

J. Jia et al., Nucl. Sci. Tech. 35, 220 (2024)

low-energy H.I. fusion reactions of a deformed nucleus

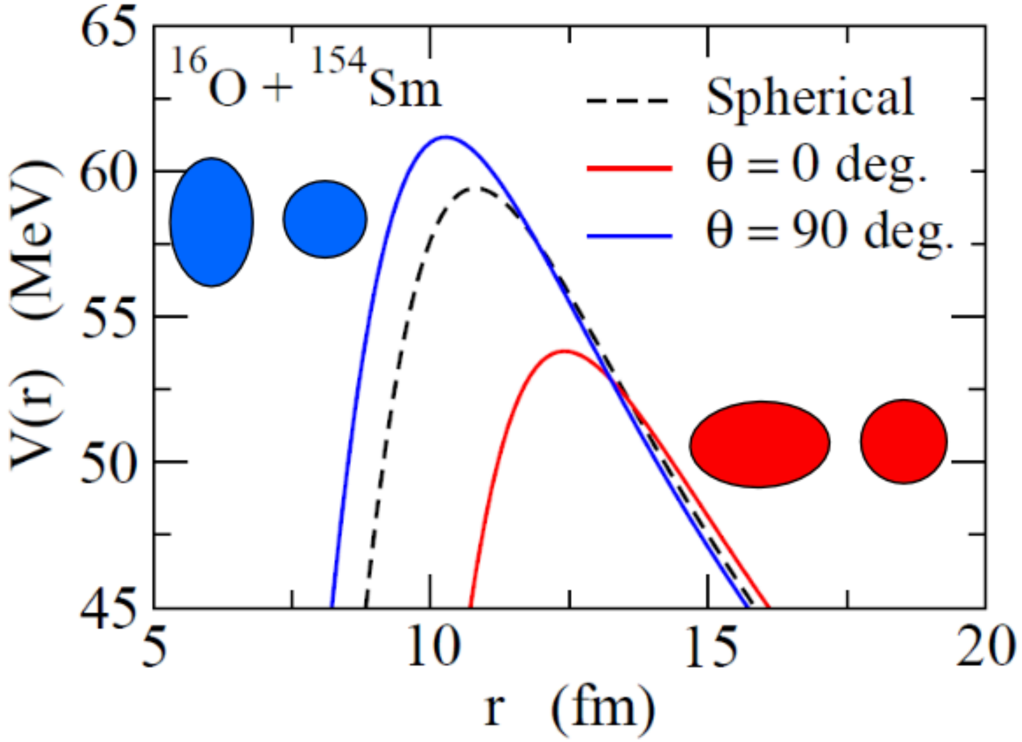

relativistic H.I. collisions with a deformed nucleus

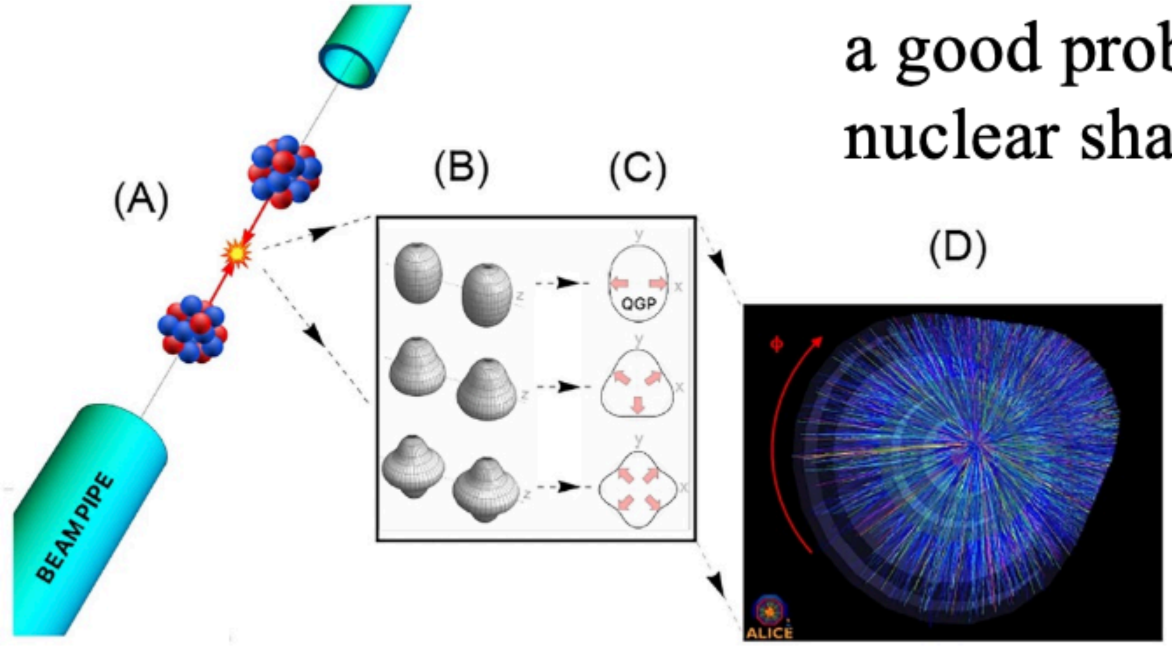

a good probe of nuclear shapes

J. Jia et al.,
Nucl. Sci. Tech. 35, 220 (2024)

increasing interests in recent years

Large similarities → intersection of **High *E*** and **Low *E*** HI collisions

Fusion reaction could be a probe to nuclei deformation.

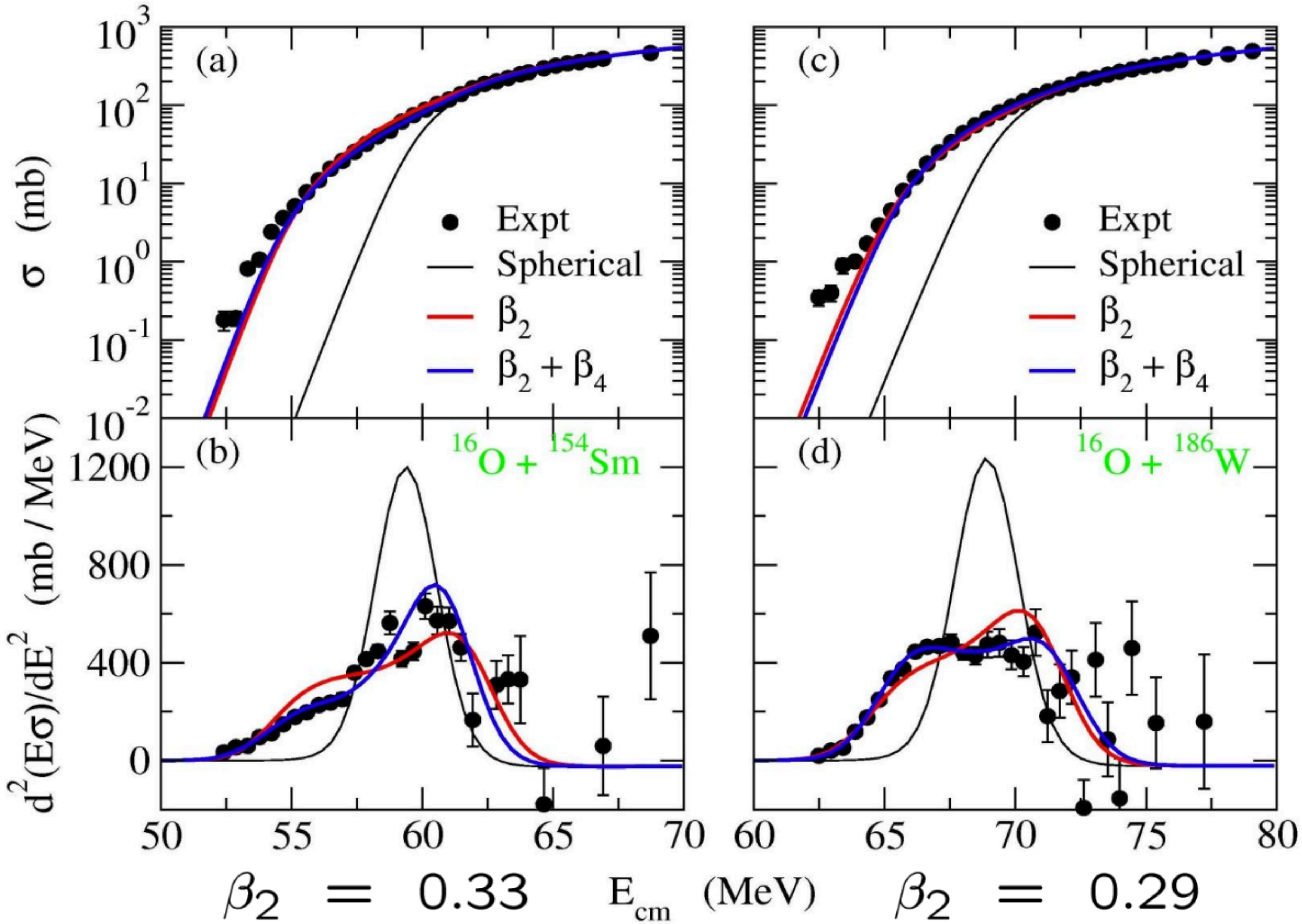

$\beta_2 = 0.33$ $\beta_4 = +0.05$

$\beta_2 = 0.29$ $\beta_4 = -0.03$

K. Hagino’ talk in INPC 2025

J.R. Leigh et al., PRC52 (‘95) 3151

Determination of hexadecapole deformation of the light-mass nucleus ^{24}Mg using quasi-elastic scattering measurements

$\beta_2 = 0.43, \quad \beta_4 = -0.11$

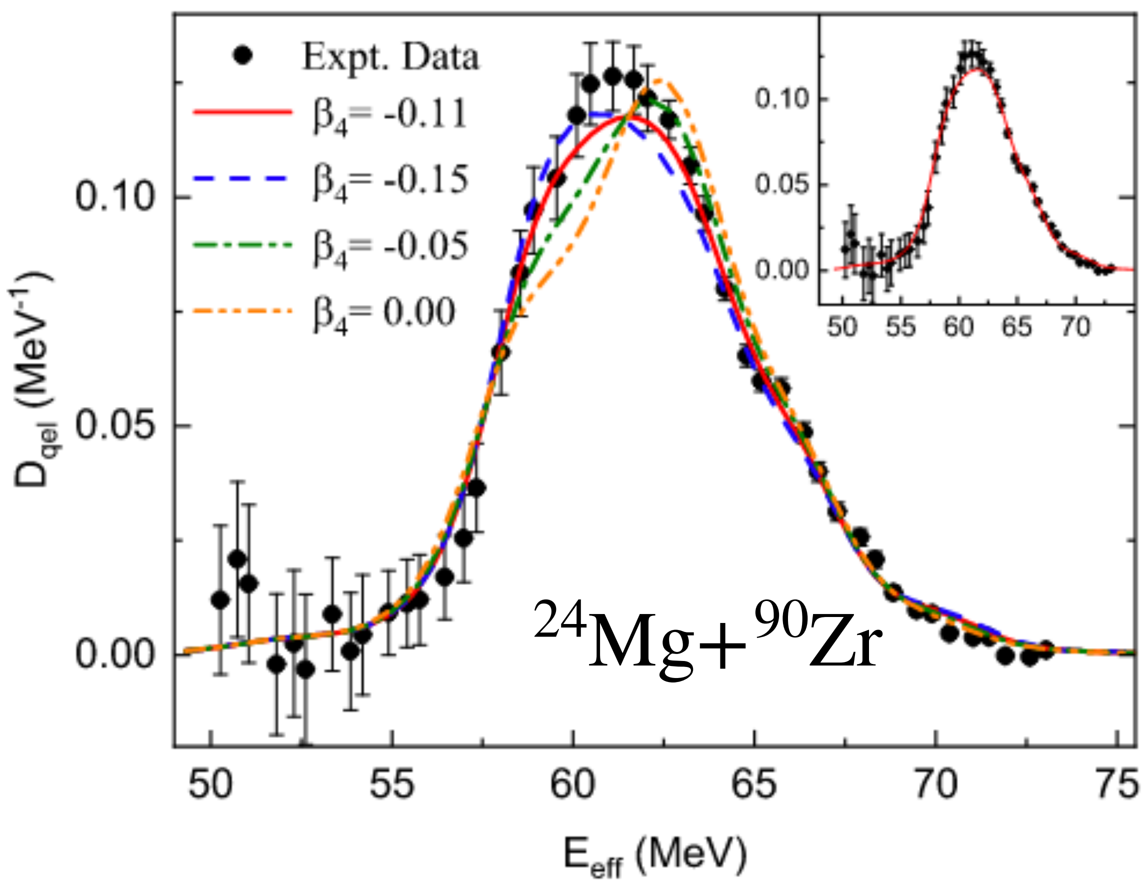

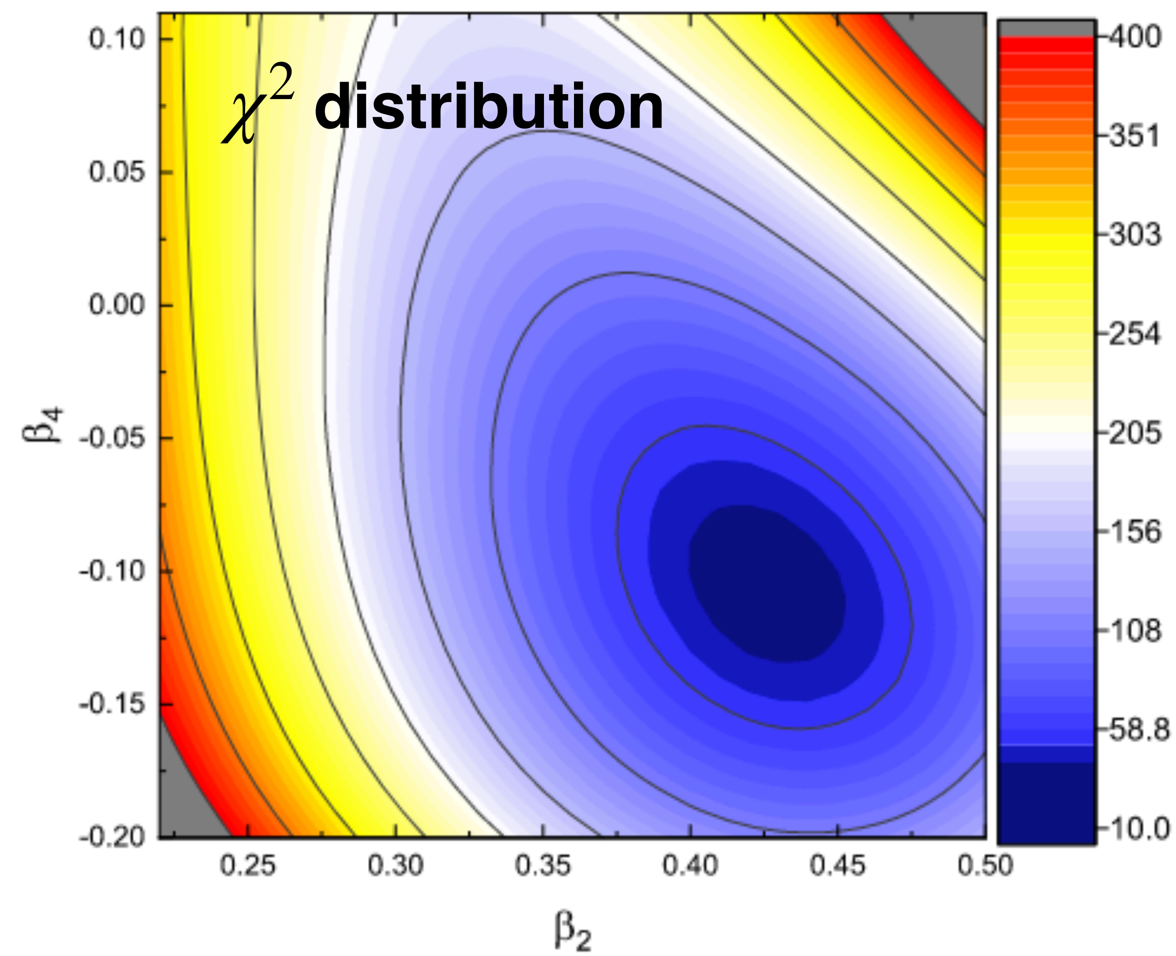

cf. (p,p’): $\beta_2 = 0.47, \quad \beta_4 = -0.05 \pm 0.08$

R. De Swiniarski et al., PRL23, 317 (1969)

$$\chi^2(\beta_2, \beta_4) = \sum_{i=1}^{N} \frac{[Y_i - f(\beta_2, \beta_4)]^2}{\sigma_i^2}$$

Y_i : **the experimental value at the i^{th} energy point,**
σ_i : **the uncertainty in the data,**
$f(\beta_2, \beta_4)$: **CCFULL calculation for a particular (β_2, β_4).**

It needs to repeat the calculation many times

Y.K. Gupta, B.K. Nayak, U. Garg, K.H., et al., PLB806, 135473 (2020)

Eigenvector Continuation：

LEC: low-energy constants (LECs) in EFT descriptions of nuclear interactions.

EC functions as a powerful emulator

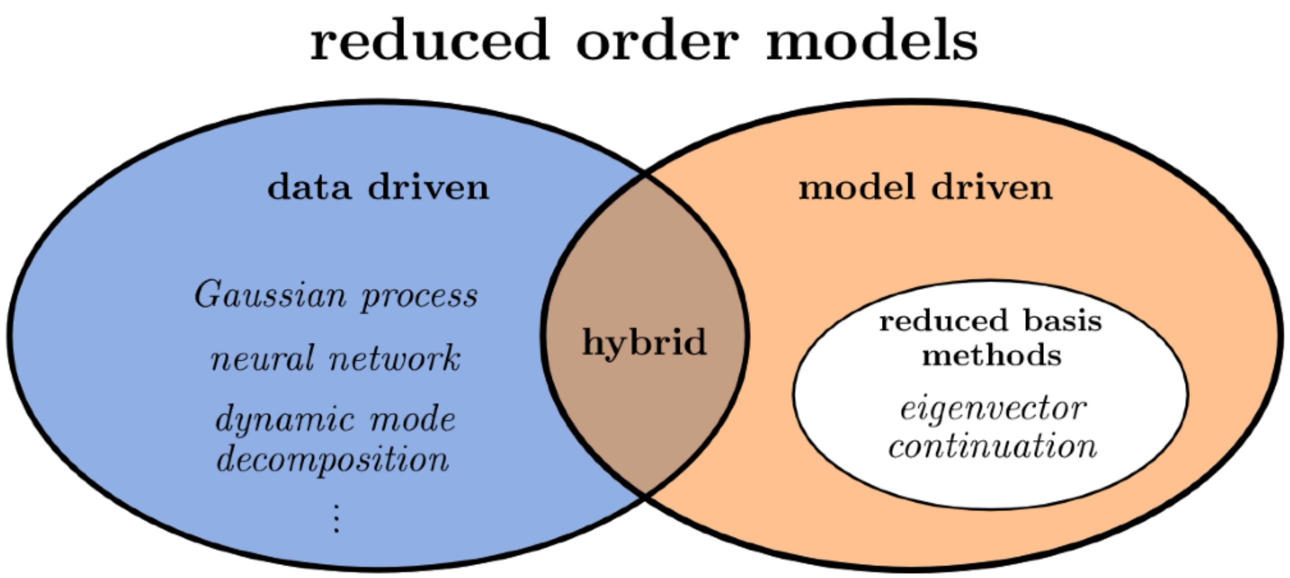

Comparison of different emulators explore a space where all 16 LECs are varied.

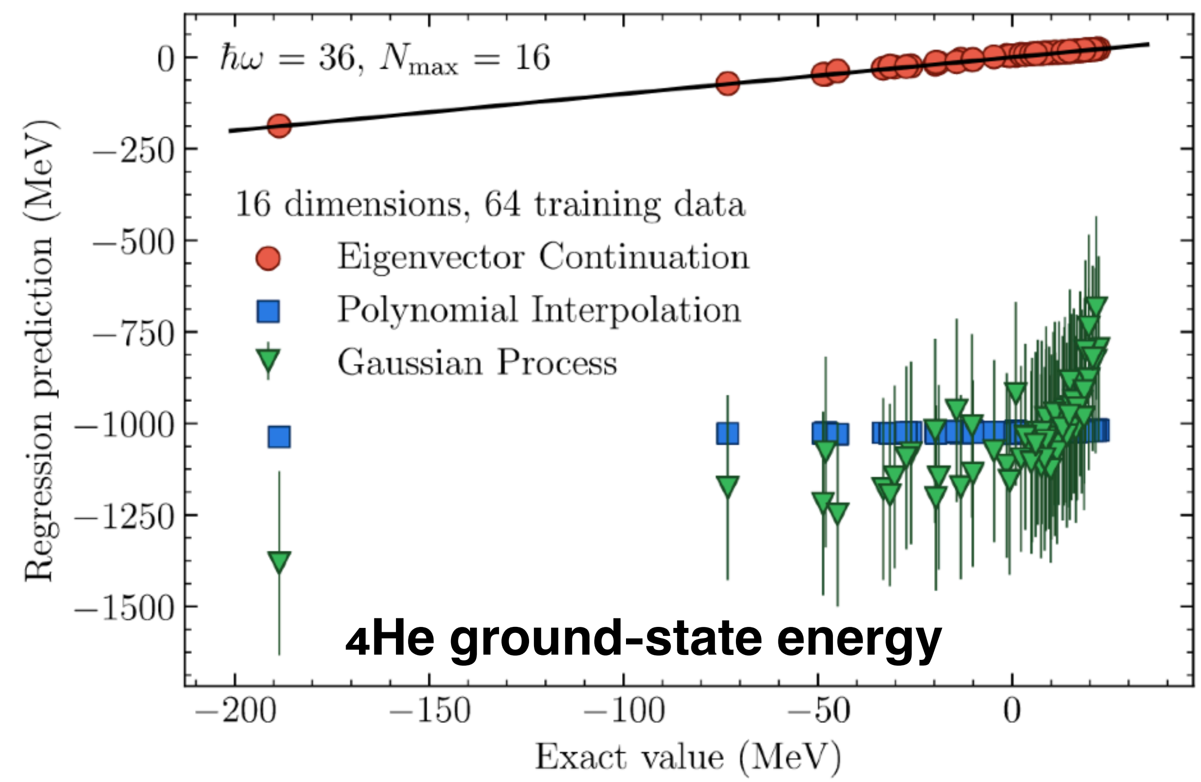

Data-driven methods:

typically interpolate the outputs of high-fidelity models without requiring an understanding of the underlying model structure

Model-driven methods

solve reduced-order equations derived from the full equations, so they are physics based and respect the underlying structure

EC is more accurate and efficient compared to established methods like Gaussian processes

Physics Letters B 810 (2020) 135814

RevModPhys.96.031002

Eigenvector Continuation：

- Select a small number of **training parameter values** θ_i. Calculate the corresponding exact eigenvectors, or **“snapshots,”**
- The EC method uses these snapshots to span a **low-dimensional variational subspace**
- For any new parameter value θ_{new}, the original large Hamiltonian $H(\theta_{\text{new}})$ is projected onto the much smaller EC subspace.
- A tiny, effective projected eigenvalue problem is solved:

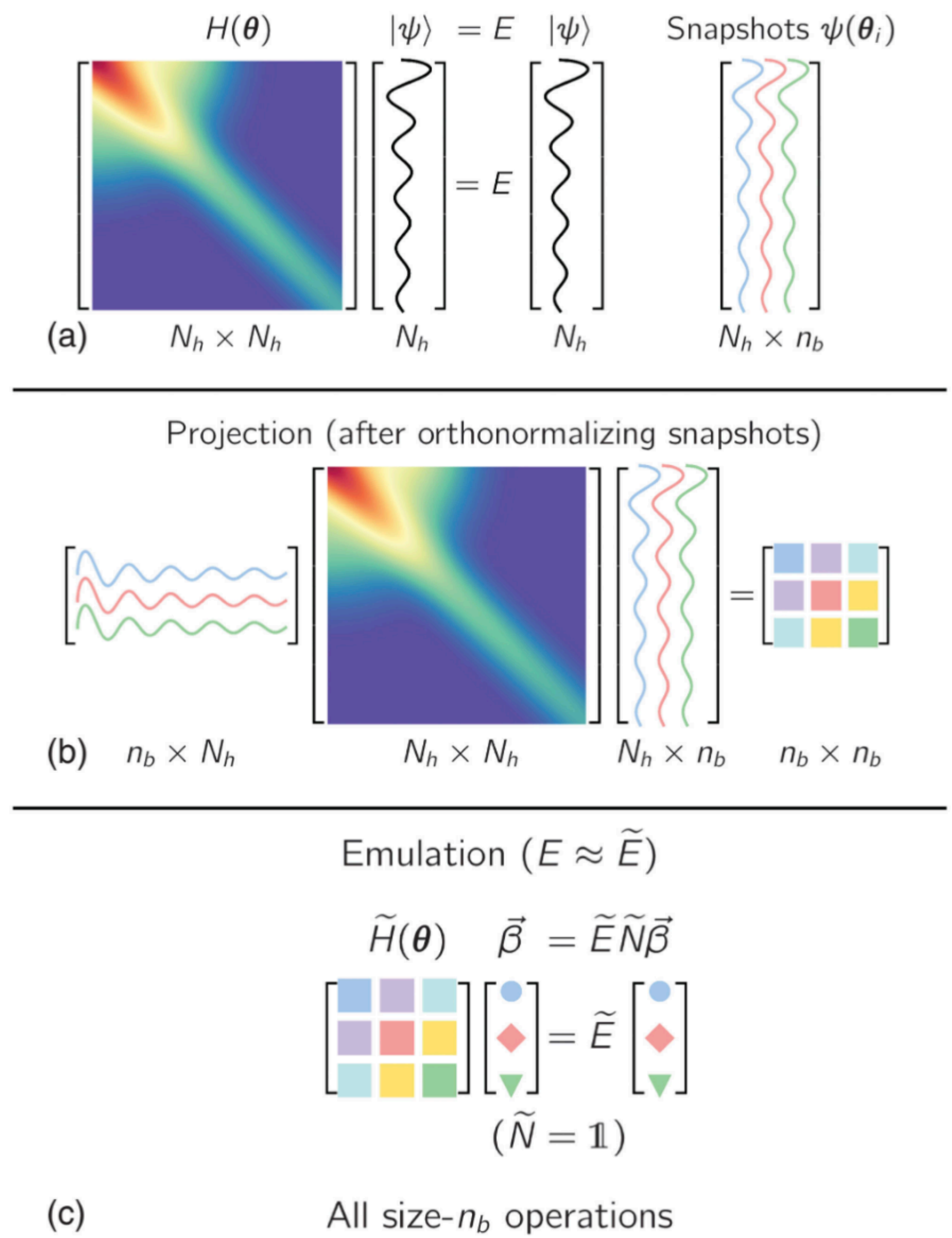

RevModPhys.96.031002

Eigenvector Continuation：

Application to no-core shell-model calculation of ^{4}He

The parameters $\boldsymbol{\theta}$ considered by König *et al.* (2020) are the low-energy constants of the chiral effective field theory (χEFT) potential used in that work. Overall, there are $d = 16$ individual parameters subsumed in $\boldsymbol{\theta}$ that determine two- and three-nucleon interactions in the potential. Setting up an EC emulator proceeds following the on-line–off-line scheme described in Sec. II for the generic RBM workflow.

(i) Picking a training set $\{\boldsymbol{\theta}_i\}_{i=1}^{n_b}$ of n_b parameters, using space-filling Latin hypercube sampling (McKay, Beckman, and Conover, 1979) in the d-dimensional parameter domain (or some subset thereof).

(ii) Performing exact calculations (for the ground states of ^{3}H and ^{4}He) in the case of König *et al.* (2020) for each point in the training set.

(iii) Constructing a pair of Hamiltonian and norm matrices as described in Sec. II for each evaluation of the emulator at a target parameter point $\boldsymbol{\theta}_*$.

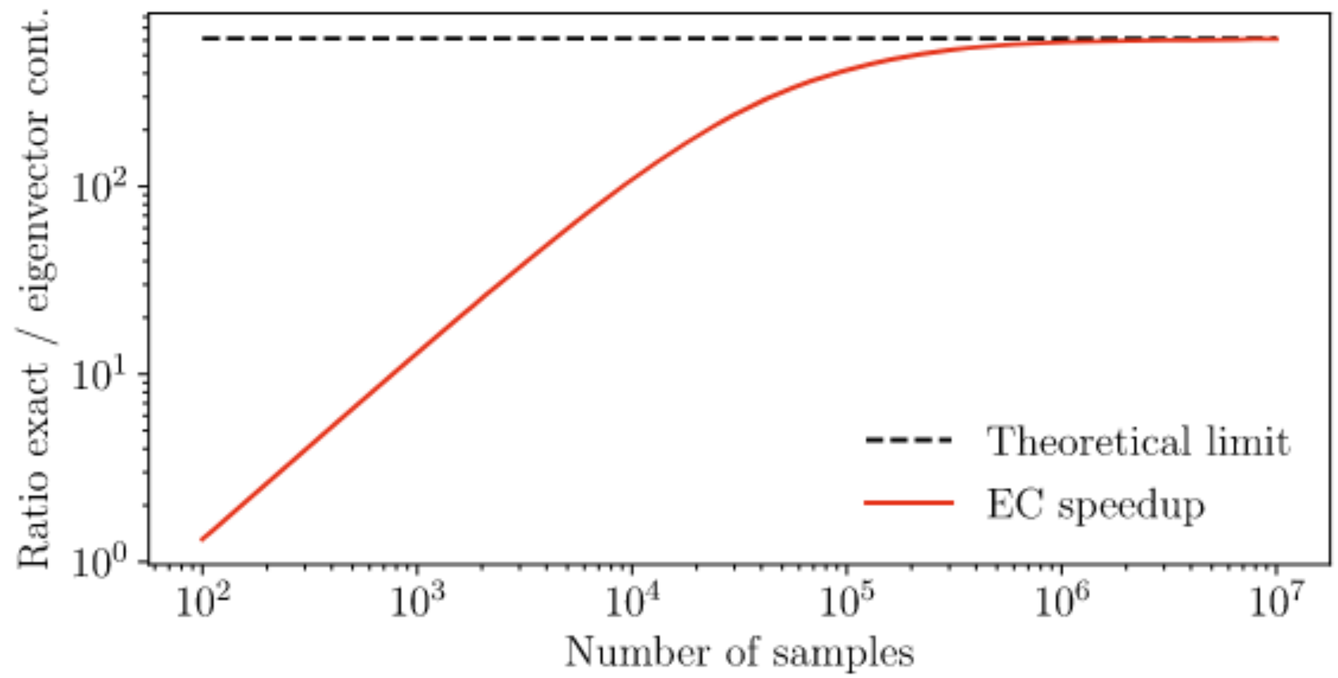

EC emulator that can be rapidly evaluated at many different parameter points. This approach achieves significant speedup factors

Konig, S., A. Ekstrom, K. Hebeler, D. Lee, and A. Schwenk, 2020, “Eigenvector continuation as an efficient and accurate emulator for uncertainty quantification,” Phys. Lett. B 810, 135814.

Emulator for Coupled Channel Model

$$H = -\frac{\hbar^2}{2\mu}\nabla^2 + V^{(0)}(r) + H_{\mathrm{int}}(\xi) + V_{\mathrm{coup}}(r,\xi)$$

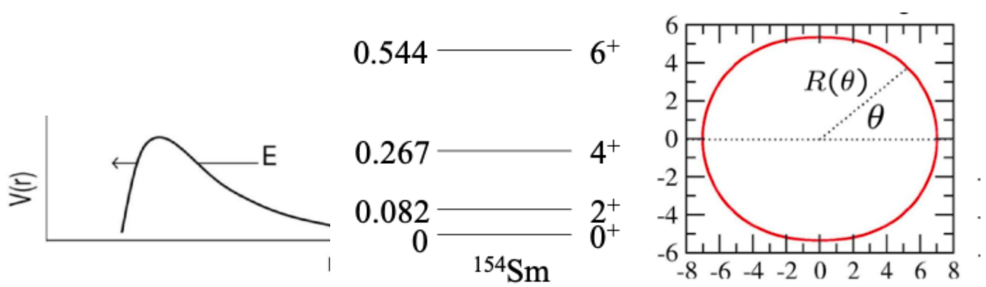

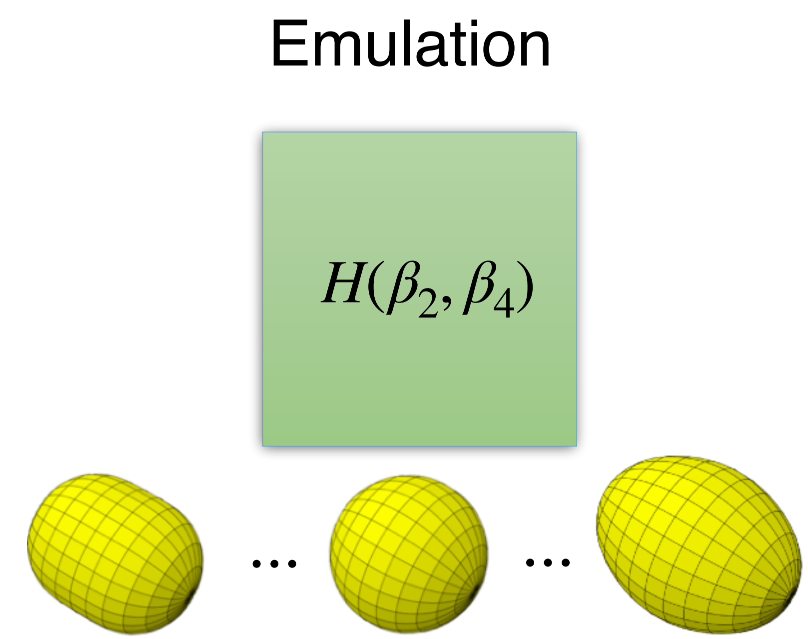

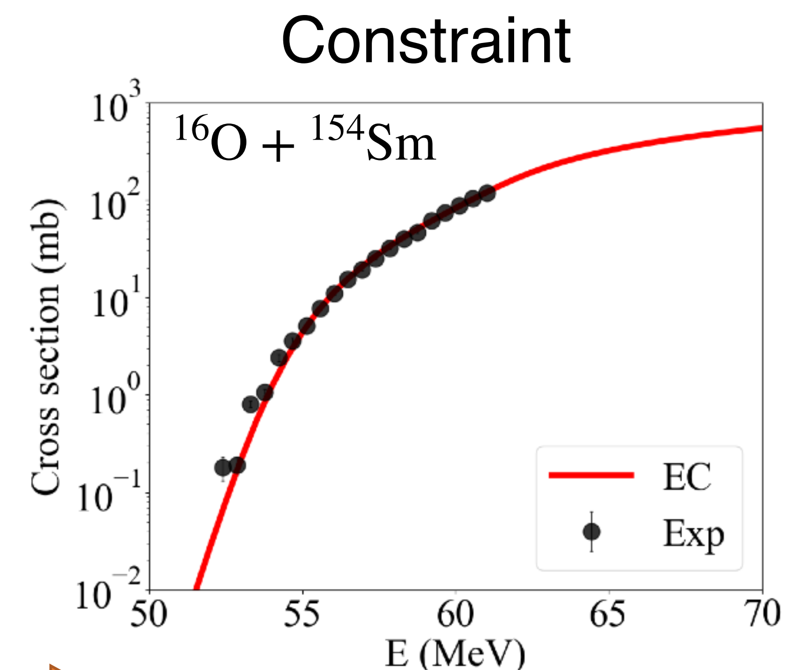

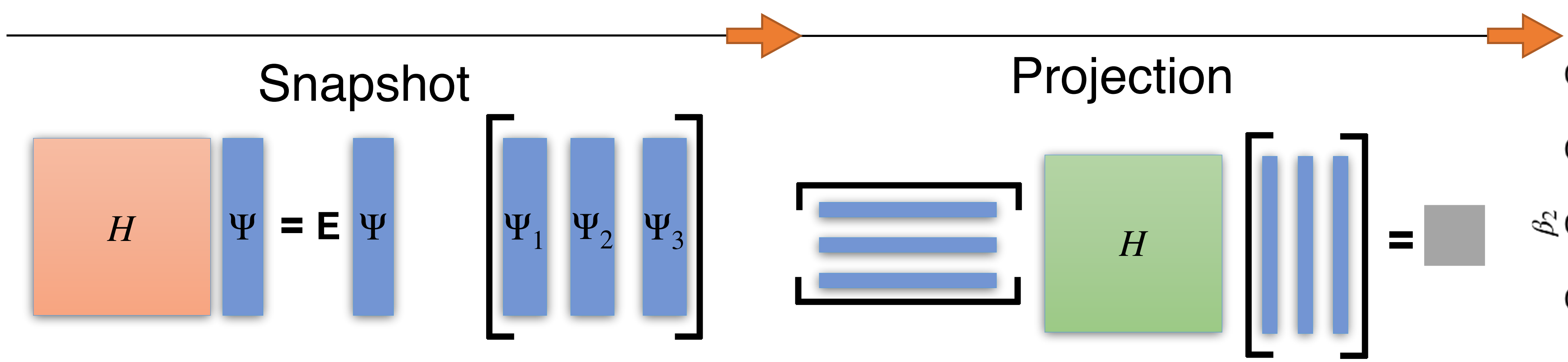

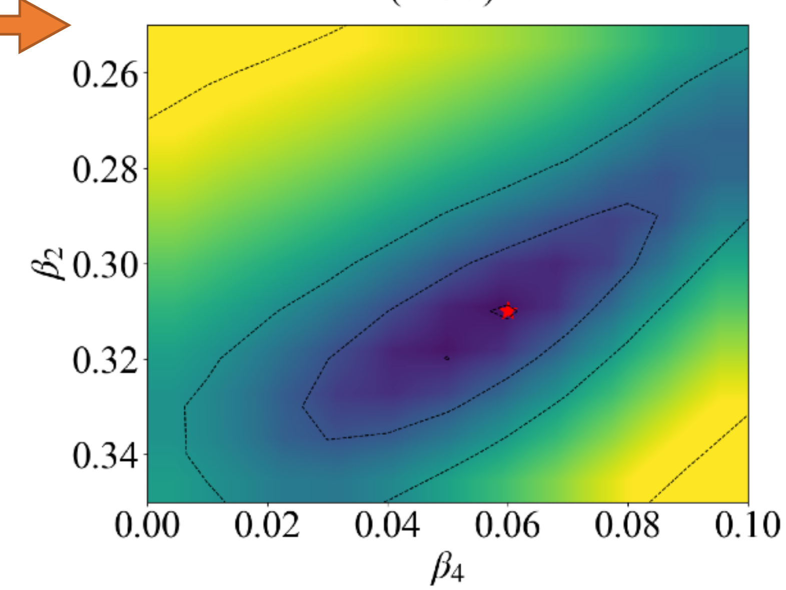

- Select a representative set of parameter points θ_i as the training set.
- Perform a small number of precise calculations
- Use these snapshots to construct the EC subspace
- The EC emulator simply uses the subspace to project the new Hamiltonian
- Solve the very small projected eigenvalue problem to obtain the approximate eigenvalues and eigenvectors **instantly**.
-

Emulator: performance

Comparison for the penetration probabilities at an energy of $E = 60\mathrm{MeV}$ across different angular momenta.

As the number N_{Channel} increases, the accelerate ability increases

As the number of basis states N_{EC} increases, the deviation from the exact result decreases.

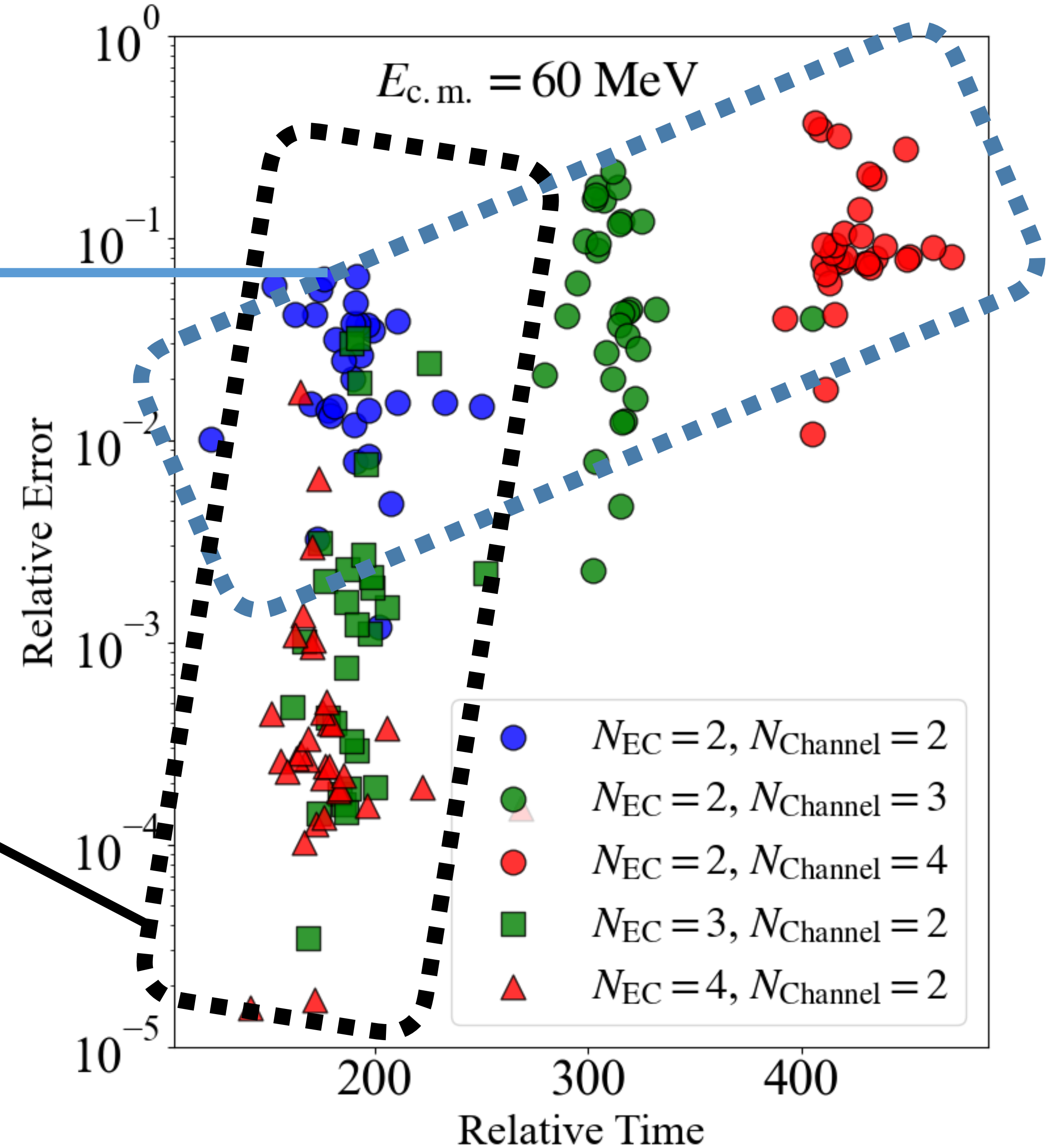

The complete space has a dimension of
~ 900 for $N_{\mathrm{Channel}} = 2$ channels
~ 1300 for $N_{\mathrm{Channel}} = 3$ channels.

Relative error = $|P_{\mathrm{Ec}}(E = 60\mathrm{MeV}, J) - P_{\mathrm{Exact}}(E = 60\mathrm{MeV}, J)|/P_{\mathrm{Exact}}(E = 60\mathrm{MeV}, J)$

Relative time = $\tau_{\mathrm{Exact}}(E = 60\mathrm{MeV}, J)/\tau_{\mathrm{Ec}}(E = 60\mathrm{MeV}, J)$

Z. Liao. et. al., in preparation

Case 1: $^{16}\mathrm{O} + ^{144}\mathrm{Sm}$

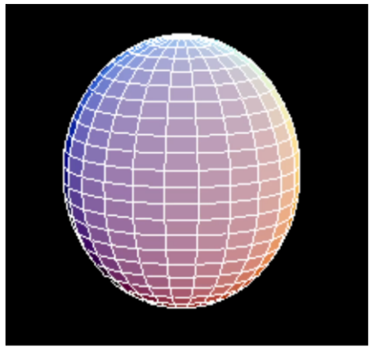

$^{144}\mathrm{Sm}$

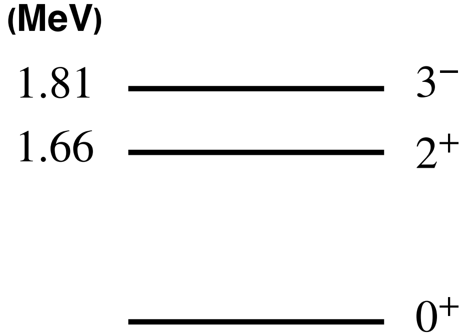

$^{144}\mathrm{Sm}$

The β^{λ} can be obtained from measured transition probability using:

$$\beta^{\lambda} = \frac{4\pi}{3ZR^{\lambda}}[\frac{B(E\lambda)}{e^2}]^2$$

cf. : $\beta_3 = 0.21$,

A.T. Kruppa et. al. Nucl. Phys. A560, 845 (1993)

CCFULL model obtained optimal strength $\beta_3 = 0.21$

The emulator Consist 5 basis

(β_3= {0.10, 0.15, 0.20, 0.25, 0.30},).

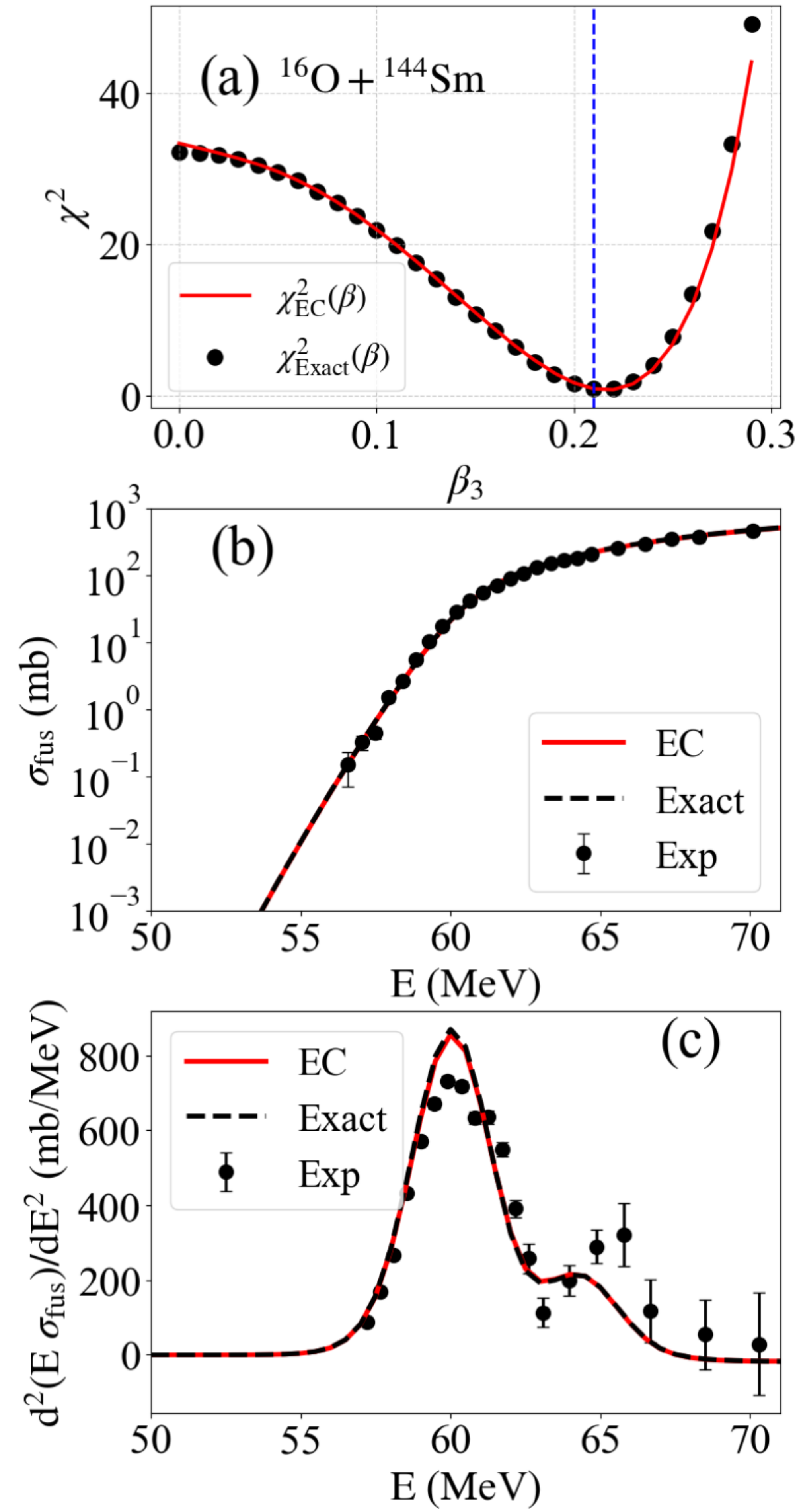

Z. Liao. et. al., in preparation

Case 2: $^{16}O + ^{154}Sm$

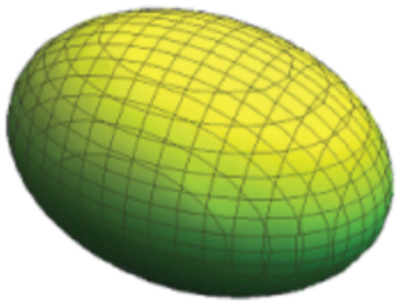

^{154}Sm

The emulator Consist 9 basis

(β_2= {0.25, 0.30, 0.35},

β_4= {0.02, 0.05, 0.08}).

CCfull Exact result: $\beta_2 = 0.31, \quad \beta_4 = 0.06$

CCfull Ec result: $\beta_2 = 0.31, \quad \beta_4 = 0.06$

re-analysis by radius parameter r = 1.06 fm

cf. (α scattering) : $\beta_2 = 0.317$ and $\beta_4 = 0.07$

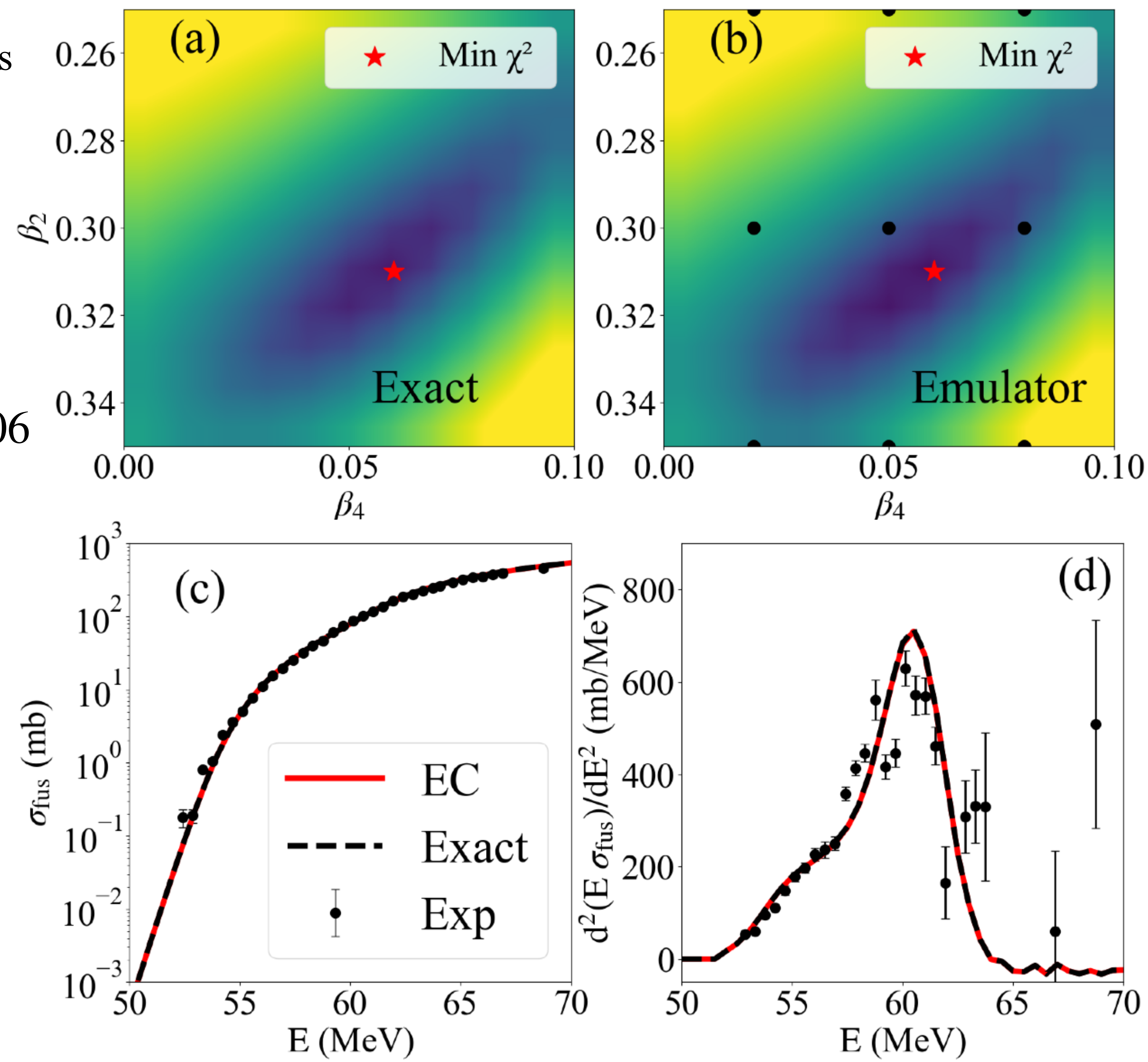

A. A. Aponik, Jr. et. al., Nucl. Phys. A159, 367 (1970).

T. Rumin, K. Hagino, N. Takigawa. Phys. Rev. C, 61, 014605

Z. Liao. et. al., in preparation

Case 3: $^{16}O + ^{186}W$

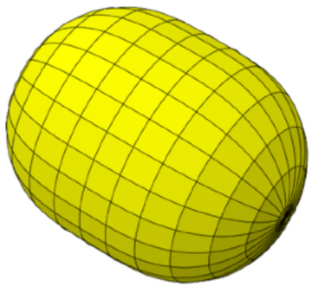

^{186}W

The emulator Consist 9 basis

(β_2= {0.25, 0.30, 0.35},

β_4= {-0.025, 0.0, 0.025}).

CCfull Exact result： $\beta_2 = 0.29, \quad \beta_4 = -0.2$

CCfull Ec result： $\beta_2 = 0.29, \quad \beta_4 = -0.2$

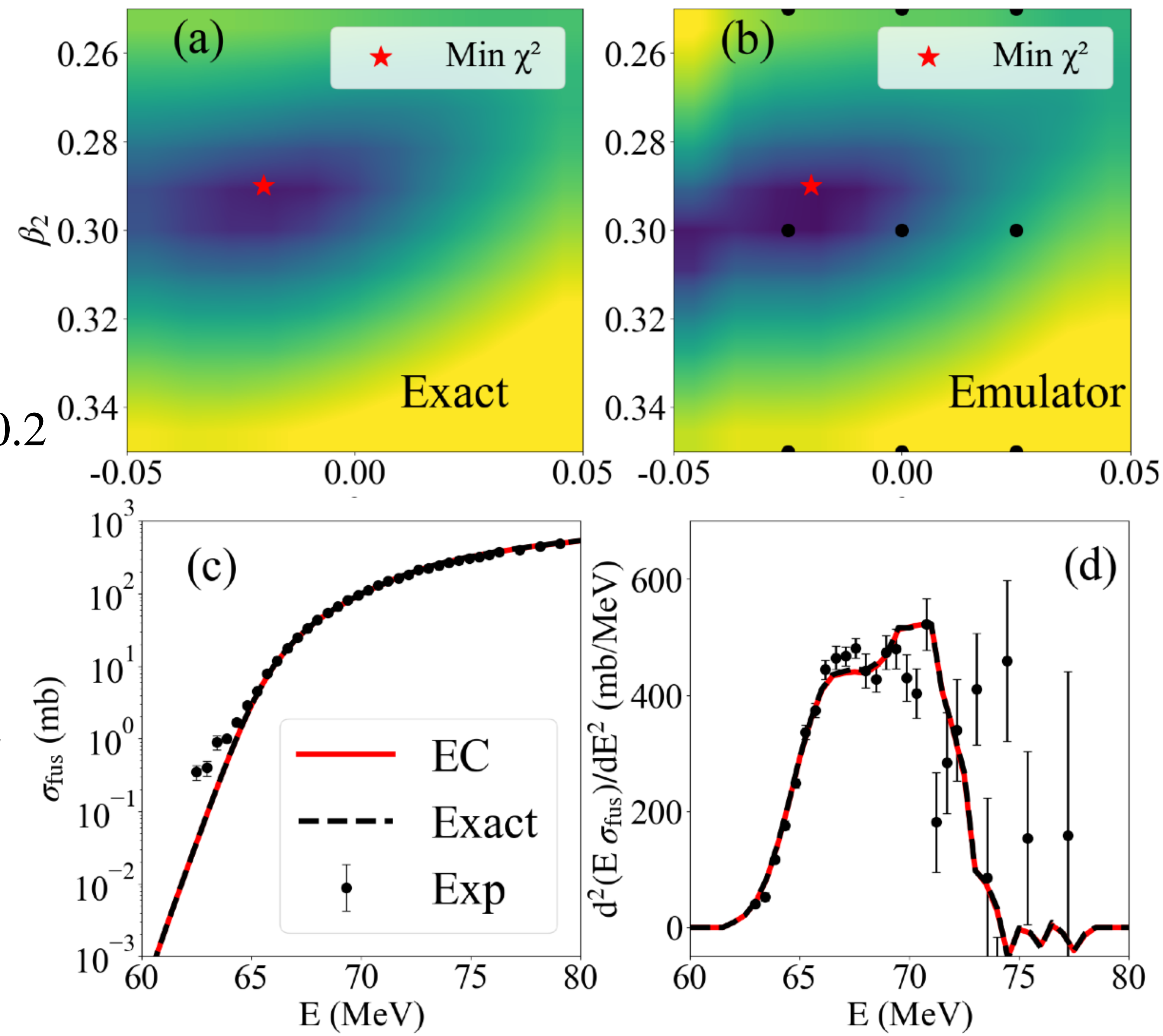

re-analysis by radius parameter r = 1.06 fm

cf. (Mass calculation) : $\beta_2 = 0.25$ and $\beta_4 = -0.117$

cf. (Neutron scattering):$\beta_2 = 0.203$ and $\beta_4 = -0.057$

tungsten

P. Moller. et. al, At. Data Nucl. Data Tables 59, 185 (1995).

J. P. Delaroche, Phys. Rev. C 26, 1899 (1982).

T. Rumin, K. Hagino, N. Takigawa. Phys. Rev. C, 61, 014605

Z. Liao. et. al., in preparation

Summary

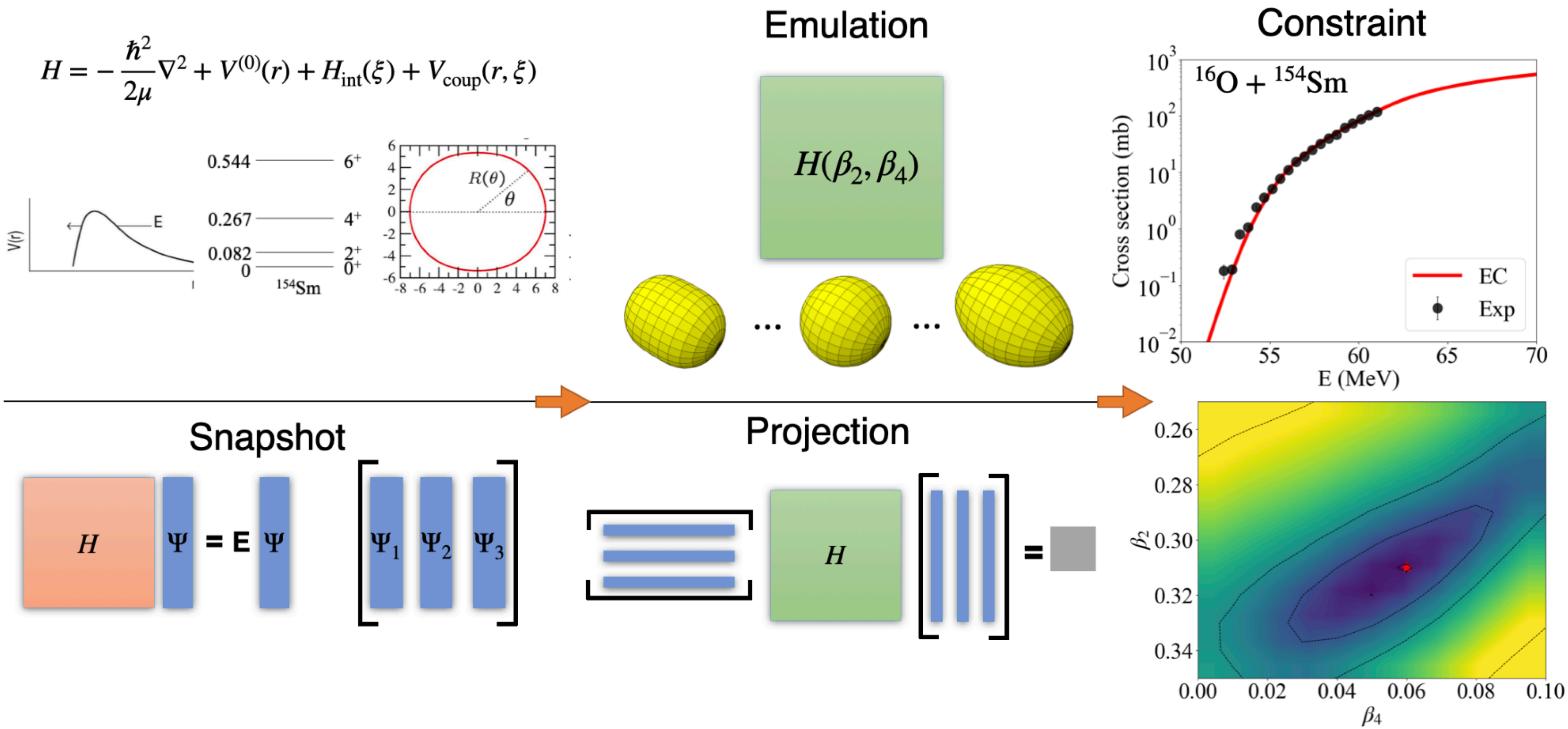

- CCFULL model can serve as a reliable theoretical tool for constraining nuclear deformation.
- We construct an emulator to accelerate this process with Eigenvector continuation

]

Z. Liao. et. al., in preparation

Future Work

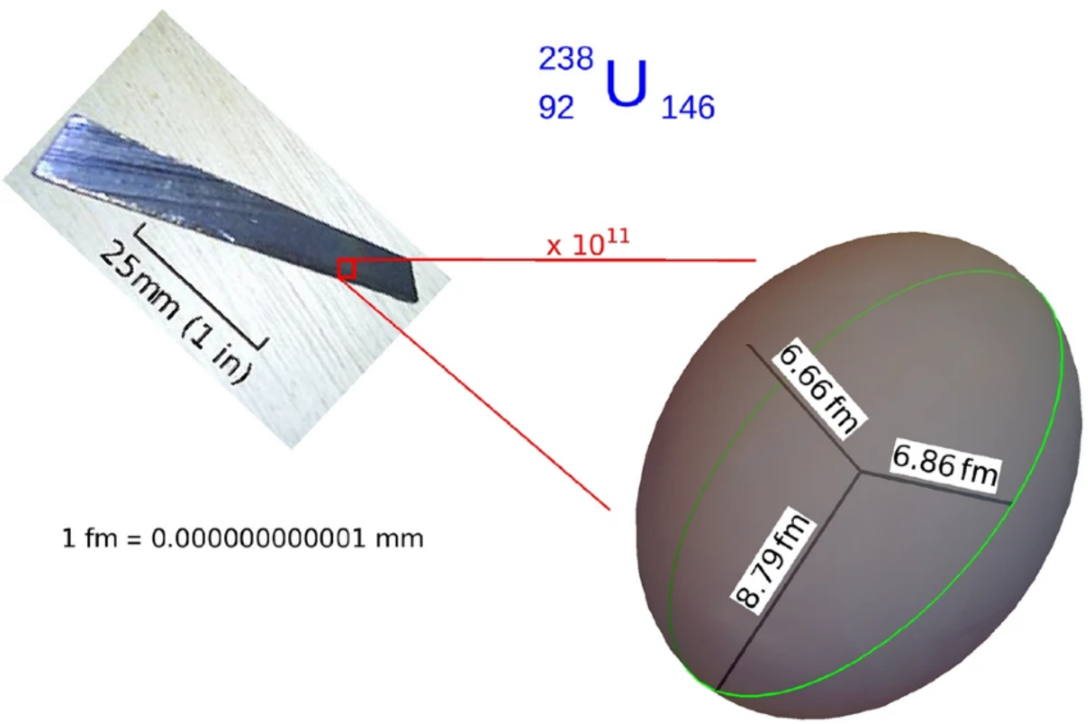

- **Uranium-238 is a typical Triaxial nuclei**
- **Triaxial deformation should be considered in CCFULL model**

$$R(\theta,\phi) = R_0\left[1+\beta_2\left(Y_2^0(\theta)\cos\gamma + Y_2^2(\theta,\phi)\sin\gamma\right)\right]$$

$$V_{\rm nm}(r_0) = V_{\rm nm}^{(C)} + V_{\rm nm}^{(N)}(r_0)$$

The nuclear coupling Hamiltonian is thus given by:

$$V_N(r, \hat{O}) = -\frac{V_0}{1 + \exp(r - R_0 - \hat{O})/a}$$

Dynamical operator: $R_0 \to R_0 + \hat{O} = R_0 + \beta_2 R_T Y_{20} + \beta_4 R_T Y_{40}$

For the matrix element of the operator $\hat{O}$, here we take one example:

Here, we know $\langle \alpha' | \beta_2 R_T Y_{20} | \alpha \rangle = \int Y^*_{j_1 m_1} \beta_2 R_T Y_{20} Y_{j_1 m_1} d\theta d\varphi$

$$\int Y_{j_1 m_1}(\theta, \varphi)\, Y_{j_2 m_2}(\theta, \varphi)\, Y_{j_3 m_3}(\theta, \varphi)\, d\Omega = \sqrt{\frac{(2j_1+1)(2j_2+1)(2j_3+1)}{4\pi}} \begin{pmatrix} j_1 & j_2 & j_3 \\ m_1 & m_2 & m_3 \end{pmatrix} \begin{pmatrix} j_1 & j_2 & j_3 \\ 0 & 0 & 0 \end{pmatrix}$$

if we only consider axi-sysmetry situation, $m_1 = 0$

$$\hat{O}_{I'0I0} = \beta_2 R_T \sqrt{\frac{5(2I+1)(2I'+1)}{4\pi}} \begin{pmatrix} I & 2 & I' \\ 0 & 0 & 0 \end{pmatrix}^2 + \beta_4 R_T \sqrt{\frac{9(2I+1)(2I'+1)}{4\pi}} \begin{pmatrix} I & 4 & I' \\ 0 & 0 & 0 \end{pmatrix}^2$$

The nuclear coupling matrix elements are then evaluated as

$$\begin{aligned} V_{nm}^{(N)} &= \langle I'0 | V_N(r, \hat{O}) | I0 \rangle - V_N^0(r) \delta_{n,m} \\ &= \sum_{\alpha} \langle I'0 | \alpha \rangle \langle \alpha | I0 \rangle V_N\left(r, \lambda_\alpha\right) - V_N^0(r) \delta_{n,m} \end{aligned}$$

$$V_{\rm nm}(r_0) = V_{\rm nm}^{(C)} + V_{\rm nm}^{(N)}(r_0)$$

The Coulomb component of the coupling Hamiltonian is evaluated as follows.

$$V_C(r) = \int dr' \frac{Z_P Z_T e^2}{|r - r'|}\rho_T(r') = \sum_{\lambda} \frac{3Z_P Z_T e^2}{(2\lambda+1)R_T^3} \sum_{\mu=-\lambda}^{+\lambda} \frac{1}{r^{\lambda+1}} Y^*_{\lambda\mu}(\hat{r}) \int_0^{2\pi}\int_0^{\pi} \frac{1}{\lambda+3} R_T^{\lambda+3}(\theta',\phi') Y_{\lambda\mu}(\theta',\phi')\, d\theta' d\phi'$$

$$R_0 \to R_0 + \hat{O} = R_0 + \beta_2 R_T Y_{20} + \beta_4 R_T Y_{40}$$

for the intergal, $\lambda = 2$**and** $\mu = 0$ **only.**

$$V_C(r) = \frac{3Z_P Z_T e^2}{5}\frac{R_T^2}{r^3}\beta_2 Y_{20}$$

Therefore, for the matrix element $V_{mn}(r)$

$$\left\langle I'0|V^C|I0\right\rangle = \left\langle I'0|\frac{3Z_P Z_T e^2}{5}\frac{R_T^2}{r^3}\beta_2 Y_{20}|I0\right\rangle + \left\langle I'0|\frac{3Z_P Z_T e^2}{9}\frac{R_T^4}{r^5}\beta_4 Y_{40}|I0\right\rangle$$

$$V_{nm}^{(C)} = V_{I0,I'0}^{(C)} = \frac{3Z_P Z_T e^2}{5}\frac{R_T^2}{r^3}\sqrt{\frac{5(2I+1)(2I'+1)}{4\pi}}\left(\beta_2 + \frac{2}{7}\sqrt{\frac{5}{\pi}}\beta_2^2\right)\begin{pmatrix} I2I' \\ 000 \end{pmatrix}^2$$
$$+\frac{3Z_P Z_T e^2}{9}\frac{R_T^4}{r^5}\sqrt{\frac{9(2I+1)(2I'+1)}{4\pi}}\left(\beta_4 + \frac{9}{7}\sqrt{\frac{1}{\pi}}\beta_2^2\right)\begin{pmatrix} I4I' \\ 000 \end{pmatrix}^2$$

Emulator: Accuracy performance

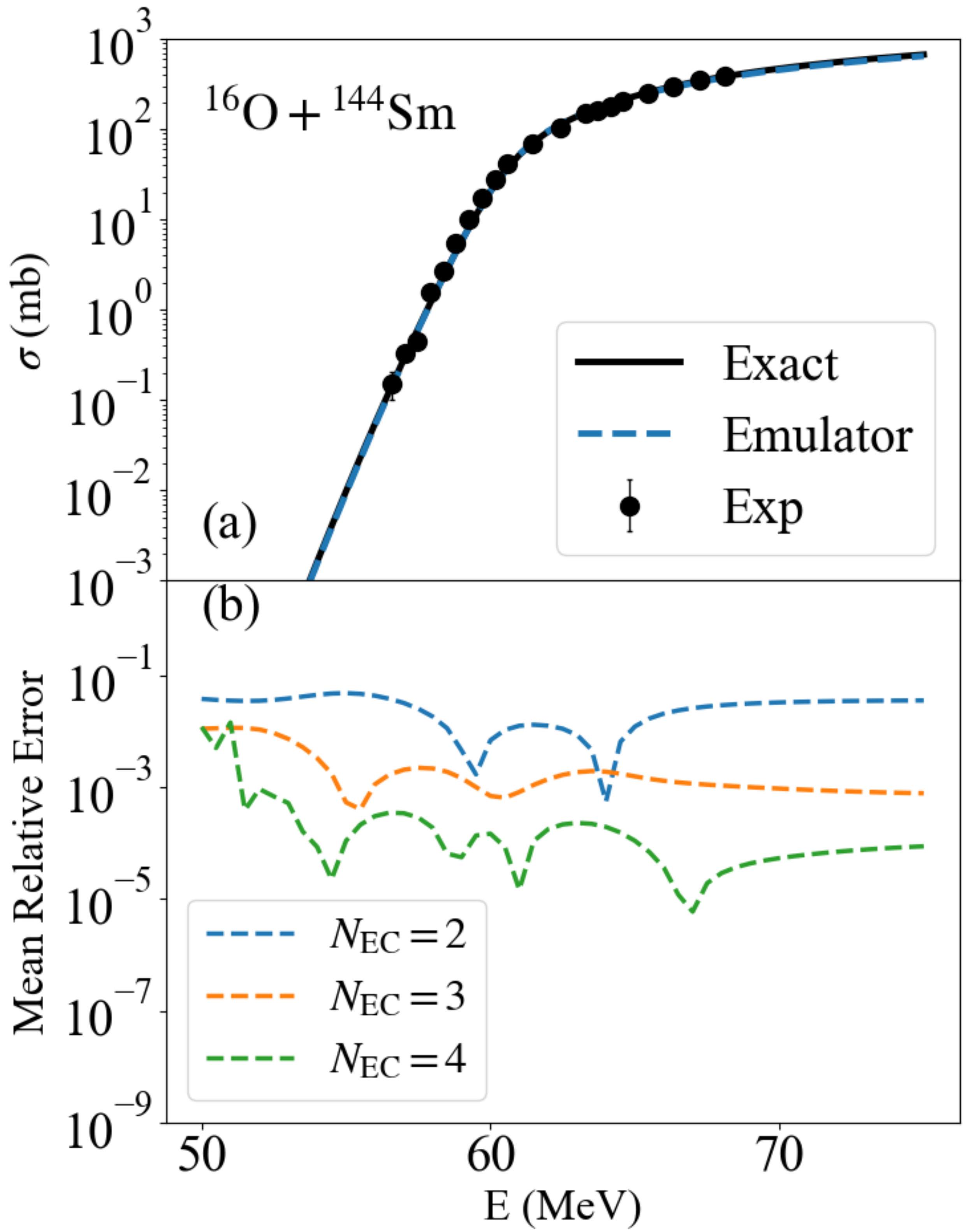

$$\epsilon = \frac{1}{N} \sum_i \frac{|\sigma^i_{\mathrm{Ec}}(E) - \sigma_{\mathrm{Exact}}(E)|}{\sigma_{\mathrm{Exact}}(E)}$$

For the exact result into ccfull model

- **The octupole vibration deformation parameter** $\beta_3 = 0.21$

For the Ec calculation, we show the case $N_{Ec} = 2$.

- **For the this case, we choose the basis** ($\beta_3^{(i)} = 0.23, 0.25$) **to emulate the exact case**

the values of β_3 **are chosen randomly in the range of (0.15, 0.25) and an ensemble average is taken for 5 different samples.**

The more basis number, The less error

Z. Liao. et. al., in preparation